Role of the unfolded protein response and ER stress in the activation of dendritic cells

Elisabeth GILIS

21 mei 2012

Elisabeth Gilis   *Professor Dr. Bart Lambrecht*

I

Foreword

This thesis represents the closure piece of a highly instructive internship in the laboratory of Immunoregulation and Mucosal Immunology of Professor Dr. Bart Lambrecht. The literature study, as well as the scientific research were the result of months of hard work, but would not have been possible without the help of many others who guided me through this process.

First of all, I would like to thank my promoter Professor Dr. Bart Lambrecht for the trust and opportunity he gave me to do my internship in this laboratory. I was surrounded by a team of researchers who were willing to share with me their remarkable knowledge and experience in the immunology.

Special thanks go to my co-promoter, Fabiola Osorio, for the excellent support, practical guidance, patience and reviewing of my thesis. She was always ready to answer my questions and to take her time whenever I had a problem. It was soon clear that I had the chance to learn from the best.

I would also like to especially thank Philippe Pouliot to guide me previous year and to be always prepared to help and give advice.

I additionally want to thank some extra people: Sophie, not only for the advice and follow-up of my thesis, but also for the friendly talks and feedback when I had to give presentations, Filipe for his help with the Nanodrop, even when he had lots of other things to do, Julie and Jessica for the many talks and support, and the technicians Sofie, Justine, Karl, Wendy, Kim and Manon for their helpfulness and the many practical and technical questions I could ask them. Besides this I want to thank all the other people of the lab (Hamida, Simon, Monique, Maud, Katrijn, Katrien, Dorine, Kaat, Nele, Lynn, Leen, Melissa, Ismé, Ruth, Jonathan, Guillaume, Martijn, Martin, Lotte, Karim and Lana) for their spontaneous help and pleasant talks.

Thanks to my friends, there was also some time for amusements during this busy year. The cozy dinners and movie nights were perfect to take a breather after a day of hard work. For that, I'm grateful to them all.

Last but not least, I would like to thank my parents and brother because they always supported and stimulated me to get the best out of myself.

This thesis would not have succeeded without the help from all these persons. Thank you!

Elisabeth

Table of contents:

Abbreviations:

APC	antigen presenting cell
APS	ammonium persulfate
ATF4	activating transcription factor 4
ATF6	activating transcription factor 6
BCR	B-cell receptor
BiP	immunoglobulin-heavy-chain-binding protein
BMDC	bone marrow-derived dendritic cell
BSA	bovine serum albumin
CCR2	chemokine (C-C motif) receptor 2
cDC	conventional dendritic cell
Cdl	curdlan
CDP	common DC progenitor
CHOP	CCAAT/enhancing-binding protein homologous protein
CLP	common lymphoid progenitor
CMP	common myeloid progenitor
CO_2	carbon dioxide
DAMP	damage-associated molecular pattern
DC	dendritic cell
ECL	enhanced chemiluminiscent
EDEM	ER degradation-enhancing a mannosidase-like protein
EDTA	Ethylenediaminetetraacetic acid
eIF2	eukaryotic initiation factor 2
ELISA	Enzyme-Linked Immuno Sorbent Assay
ER	endoplasmic reticulum
ERAD	ER-associated protein degradation
ERSE	ER stress responsive elements
FCS	fetal calf serum
GADD34	growth arrest and DNA damage-inducible 34
GAPDH	glyceraldehyde 3-phosphate dehydrogenase
GM-CSF	granulocyte-macrophage colony-stimulating factor
HBSS	Hanks' Balanced Salt Solution
HDM	house dust mite

HEPES	(4-(2-hydroxyethyl)-1-piperazineethanesulfonic acid
HSC	hematopoietic stem cell
iDC	inflammatory dendritic cell
IFN	interferon
Ig	Immunoglobulin
IL	interleukin
iNOS	inducible nitric oxid synthetase
IRE1	Inositol-requiring protein-1
LC	langerhans cells
LN	lymph node
LPS	lipopolysaccharide
MDA-5	melanoma differentiation-associated protein 5
MDP	macrophage-DC progenitor
MHCII	major histocompatibility complex
NK	natural killer
NLR	NOD-like receptor
ORF	open reading frame
PAMP	pathogen-associated molecular pattern
PCR	polymerase chain reaction
pDC	plasmacytoid dendritic cell
PERK	protein kinase-like ER kinase
pre-DC	precursor of dendritic cells
PRR	pathogen recognition receptor
qrt-PCR	quantitative real-time polymerase chain reaction
RBC	red blood cell
RLR	RIG-I like receptor
RPMI	Roswell Park Memorial Institute
RT	room temperature
S1P	site-1 protease
S2P	site-2 protease
SDS	sodium dodecyl sulfate
TBE	Tris-Borate-EDTA
TBS	Tris-buffered saline

TCM	tissue culture medium
Th1	type 1 helper T-cells
Th2	type 2 helper T-cells
TLR	toll-like receptor
TNF	tumor necrosis factor
Treg	regulatory T cell
Tun	tunicamycin
UPR	unfolded protein response
WT	wild type
XBP1	X-box binding protein 1
XBP1s	XBP1 spliced
XBP1u	XBP1 unspliced

Abstract

Endoplasmic reticulum (ER) stress results from perturbations that compromise the protein folding capacity of the ER and lead to the accumulation of unfolded proteins. To survive the stress, cells activate the unfolded protein response (UPR) which adjusts transcriptional and translational processes to the current protein folding state. By alleviating the biosynthetic load and stimulating the folding capacity of the ER, ER stress is diminished. The UPR consists of three ER stress sensors of which IRE1 is the most conserved. It activates the transcription factor XBP1 to eventually up-regulate ER stress related genes, such as chaperones. Interestingly, XBP1 has been found to be essential for the development and survival of plasmacytoid and conventional dendritic cells (DCs), a feature that had only been described for plasma cells and highly secretory cells.

In this thesis, the role of XBP1 in DC survival, maturation, function and ER stress management was investigated. The CD11c Cre-LoxP system was used to generate a mouse model with a specific deletion of *Xbp1* in DCs and inflammatory DCs (iDCs) were generated from cultured bone marrow cells in the presence of the growth factor granulocyte-macrophage colony-stimulating factor (GM-CSF). To promote survival, iDCs were stimulated with distinct pathogen recognition receptor (PRR) ligands. Additionally, the capacity of these PRR-stimuli to trigger ER stress in iDCs was assessed.

Our results demonstrate an inter-connection between specific PRR-pathways and the UPR in iDCs, as stimulation with lipopolysaccharide (LPS), house dust mite (HDM), CpG oligodeoxynucleotides and curdlan induced up-regulation of ER stress markers. A crucial role for XBP1 in iDC survival could not be demonstrated, since the frequencies of alive cells were only mildly decreased in XBP1-deficient iDCs. Additionally, expression of co-stimulatory molecules (CD40, CD86), indicating maturation status, did not appear altered in XBP1-deficient iDCs. This excludes a key role for XBP1 in iDC maturation, although the capacity of iDCs to secrete cytokines, which also provides an indication for normal maturation, did show differences between the two groups. More specifically, PRR-stimulated iDCs secreted lower levels of cytokines in the absence of XBP1. This effect was ligand- and cytokine-specific, with IL-6 and IL-12 being the most affected in response to LPS and HDM. Finally, an imbalance in ER stress was observed in absence of XBP1 as noted by the up-regulation of BiP at baseline, indicating that XBP1 is essential for the maintenance of homeostasis in the ER.

In general we could conclude from this thesis that the IRE1-XBP1 pathway is relevant for the sensing of noxious stimuli in iDCs.

1   Introduction

1.1   Immune system

Our body is constantly exposed to microorganisms of which many are able to cause disease. However, most of the time diseases do not succeed and we rarely become ill. This is because of our immune system, which functions to protect our body against all kinds of threats including infections, autoimmunity and cancer. The first line of defense against microorganisms consists of physical and/or chemical barriers that prevent pathogens from entering the body, including the skin, mucous membranes, stomach acids and destructive enzymes in secretions (1, 2). Importantly, the skin also constitutes a crucial part of this system as it contains molecules with microbicidal activity such as defensins (3). Once microorganisms have trespassed this barrier, the immune system comes into play.

The immune system consists of two arms that are activated sequentially. The first arm of defense, the innate immune system, is an evolutionarily conserved mechanism that arises quickly and comprises various cell types such as mast cells, granulocytes (including basophils, eosinophils and neutrophils), macrophages, dendritic cells and natural killer cells, all of which express pattern recognition receptors (PRRs) (2, 4). Importantly, these receptors recognize conserved molecular patterns present on micro-organisms, called pathogen-associated molecular patterns (PAMPs), but also molecules released by injured host cells, which are termed danger-associated molecular patterns (DAMPs) (5). Upon detection, innate immune cells engulf (through a process called phagocytosis) and kill invading microorganisms. To make this process more efficient, these cells release chemokines that attract other immune cells, leading to an augmentation of phagocytic cells at the site of infection. Apart from this phagocytic function, innate immune cells also secrete granules which contain a variety of enzymes and toxic proteins, rendering them competent to destruct the invading pathogen directly (1). However, one of the main functions of the innate immune system is to activate adaptive immunity by translating innate into adaptive response, *via* secretion of chemokines and cytokines among others (6). When the innate immune system is not able to overcome the current infection, help is offered by the adaptive immune system. This system relies on T- and B-cells of which each cell is equipped with a structurally unique receptor on its surface. The total repertoire of T- and B-cells in one individual is big enough to be able to recognize virtually any pathogen that could be encountered during a person's lifetime (2, 7). Upon binding of an antigen to a cognate B-cell receptor (BCR), the B-cell proliferates and differentiates into its effector form, namely plasma cells. These cells produce

large amounts of antibodies which represent the soluble form of the BCR. Antibodies produced in this T-cell-independent way, have low antigen-affinity and are of the immunoglobulin M (IgM) isotype. They also lack memory response seen upon re-exposure to the same antigen (8). In order to produce high-affinity antibodies with a wide spectrum of isotypes (especially the IgG isotype), B- and T-cells should be activated simultaneously by the same insult. In this context, CD4 T-cells differentiate into type 2 helper T-cells (Th2) that are able to provide help in the activation of B-cells, which is needed for defenses against extracellular micro-organisms (2). The type 1 helper T-cells (Th1) on the other hand, provide help in fighting intracellular threats *via* the secretion of interferon-γ (IFNγ) and activation of macrophages (9). Other than T helper cells, T-cells can also differentiate into cytotoxic T-cells and regulatory T-cells (Treg) upon activation. In contrast to B-cells, T-cells are not directly activated upon exposure to the antigen. Instead, the antigen needs to be processed and presented by an antigen presenting cell (APC) in the context of major histocompatibility complex (MHC) molecules and co-stimulatory signals such as CD80 and CD86 (1). Activation of APCs is therefore crucial to induce an efficient adaptive immune response. This brings us to the cells we are highly interested in as they bridge the innate and the adaptive immune system, namely dendritic cells (DCs).

1.1   Dendritic cells

DCs are specialized APCs that are characterized by following features (figure 1): 1) they are equipped with distinct PRRs such as toll-like receptors (TLRs), RIG-I like receptors (RLRs), NOD-like receptors (NLRs) and C-type lectin receptors (CLRs) (10). Each type of these PRRs detects a unique pattern that is conserved among different micro-organisms or cells. Gram negative bacteria for example, are recognized by TLR4 *via* the presence of lipopolysaccharide (LPS) in their cell-wall (11). RIG-I like receptors on the other hand, detect dsRNA which is characteristic of some set of viruses (4). Additionally, injured cells can also release DAMPs which activate DCs as well upon binding to PRRs. 2) After pathogen and/or danger sensing, DCs become effector cells that engulf the antigens and process them into peptides. 3) Effector DCs have the capacity to migrate to the lymph nodes, a quality that is crucial since antigen-capture takes place at the site of infection, whereas presentation to the antigen-specific T-cells occurs at the draining lymph nodes. 4) When arrived in the lymph nodes, they present the peptides to naïve T-cells in the context of MHC class I or II molecules. In addition, T-cell activation requires a second signal delivered from co-stimulatory molecules on the DCs (CD40, CD80 and CD86) but also a third signal that is

provided *via* the secretion of cytokines. Importantly, the type of cytokine that is released by the DCs, determines the quality of the adaptive immune response. More specifically, IL-12 secretion induces Th1 cells (12), while IL-10 and IL-6 secretion polarizes the T-cells toward a Th2 phenotype (13). IL-10 additionally stimulates the induction of Treg cells (13, 14). After a period of proliferation and differentiation, the activated lymphocytes leave the lymph nodes via the efferent lymphatic vessel, which conduces them to tissues where their effector action is required (15).
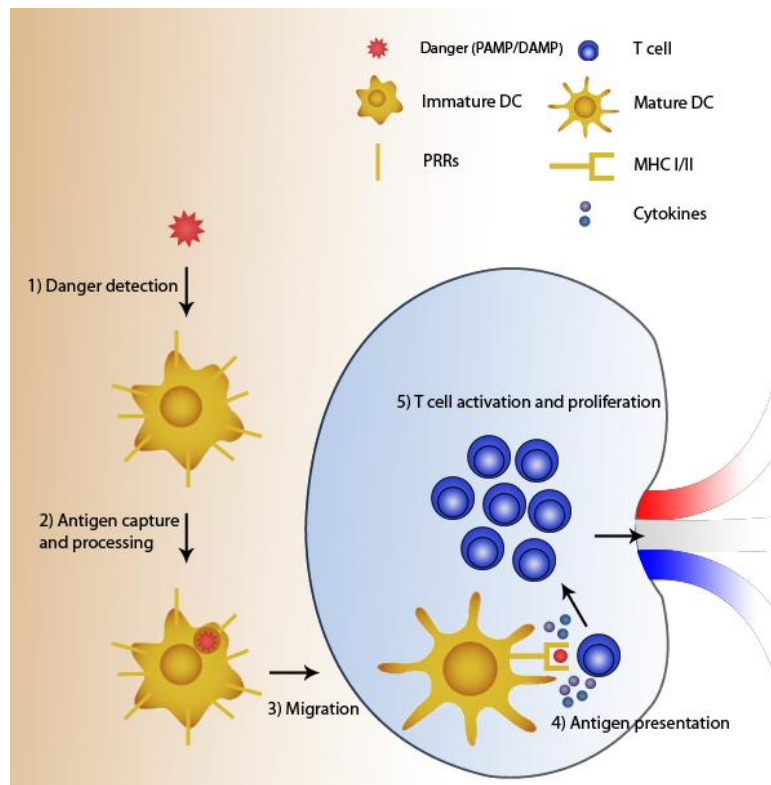

Figure 1: Life cycle of dendritic cells, the cells that bridge innate and adaptive immunity. 1) Dendritic cells (DCs) detect danger with pathogen recognition receptors (PRRs) which recognize unique patterns that are conserved among different micro-organisms, called pathogen-associated molecular patterns (PAMPs), but also damage-associated molecular patterns (DAMPs) that are released by injured cells. 2) Detection of danger is followed by capture and processing of the antigens to peptides. 3) DCs subsequently migrate to the draining lymph nodes, 4) where they present the processed antigens in the context of major histocompatibility complex class I or II molecules (MHC I/II) to naïve T-cells. 5) To activate T-cells, they require a second signal delivered from co-stimulatory molecules on the DCs (CD40 and CD86, not represented on figure) and a third signal *via* secretion of cytokines by DCs. T-cell activation is followed by proliferation and migration to the tissues where action is required. Adapted from Murphy *et al.* (2).

DC development begins in the bone marrow from pluripotent hematopoietic stem cells (HSCs) that are able to differentiate in any cell type of the myeloid and lymphoid lineage

(figure 2). The common myeloid progenitor (CMP) that arises from this stem cell is more restricted in its capacity to differentiate and is able to give rise to granulocytes, monocytes, megakaryocytes, erythrocytes and DCs (the common lymphoid progenitors, CLP, differentiate into B-, T- and NK cells). Studies have also revealed a lymphoid origin for some subsets of DCs, albeit most of the DCs are of myeloid origin (16). Further in development, a common precursor for monocytes, macrophages and DCs, termed macrophage-DC progenitor (MDP) arises and is no longer able to differentiate into granulocytes. This progenitor subsequently diverges into a monocyte and DC lineage. The latter is represented by the common DC progenitor (CDP) that further differentiates into plasmacytoid DCs (pDCs) and into precursors of DCs (pre-DCs). Monocytes give rise to macrophages and inflammatory DCs (iDCs) in conditions of inflammation (17, 18).
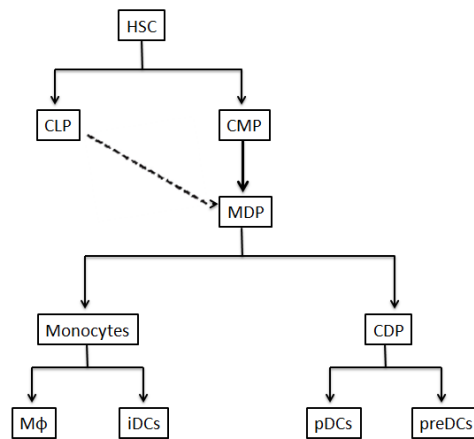

Figure 2: Development of dendritic cells (DCs) from hematopoietic stem cells (HSCs). HSCs in the bone marrow have the capacity to differentiate into common lymphoid progenitors (CLPs) and common myeloid progenitors (CMPs), respectively representing the lymphoid and myeloid lineage. CLPs further differentiate in B-, T- and NK cells, although some subsets of DCs can also originate from this progenitor. CMPs on the other hand give rise to macrophage-DC progenitors (MDPs), which can diverge into monocytes and common DC progenitors (CDPs). These CDPs can finally differentiate into plasmacytoid DCs (pDCs) and into precursors of DCs (pre-DCs). In conditions of inflammation, macrophages (mφ) and inflammatory DCs (iDCs) can arise from monocytes. Adapted from Liu *et al.* (18).

Collectively, DCs form a very heterogeneous group comprised of distinct subtypes, although they all share features involved in antigen processing and T-cell activation. The distinct DC subtypes can be differentiated in view of their surface marker expression, origin, location and function. They form a highly complex network, but to start in simplicity, DCs can be divided into five main subtypes: two types of conventional DCs (cDCs) (migratory and lymphoid cDCs), Langerhans cells (LCs), pDCs and monocyte-derived DCs (iDCs) (19).

1.1.1 Conventional DCs

Conventional DCs (cDCs) are those that arise from pre-DCs, whereas pDCs and iDCs are classified as non-conventional DCs. Migratory cDCs transit from peripheral tissues to the lymph nodes and include DCs found in the skin, liver, lung, intestinal tract and kidneys. This subset is briefly discussed in a separate section. In contrast, lymphoid cDCs reside throughout their life cycle in lymphoid organs such as lymph nodes, spleen and thymus. This type of DCs has been further divided into three groups based on the differential expression of CD4 and CD8, namely $CD8\alpha^+ CD4^-$, $CD8\alpha^- CD4^+$ and $CD8\alpha^- CD4^-$ DCs (20). The two groups that lack $CD8\alpha$ expression are characterized by the expression of CD11b and are collectively designated $CD11b^+$ cells (20). In addition to displaying different markers, the $CD11b^+$ and $CD8\alpha^+$ cells perform distinct functions in the immune system. For instance, $CD8\alpha^+$ DCs are able to cross-present viral antigens to $CD8^+$ T-cells, whereas $CD11b^+$ DCs present their acquired antigens to $CD4^+$ T-cells (21, 22). $CD8\alpha^+$ DCs are also capable of inducing peripheral self-tolerance by cross-presenting self-proteins to $CD4^+$ and $CD8^+$ T-cells in the absence of infection (18, 23, 24). Cross-presentation is the process in which exogenous antigens are delivered on MHC class I molecules for antigen presentation to $CD8^+$ T-cells. Additionally, differences in cytokine production capacities are observed. When $CD8\alpha^+$ DCs are stimulated with a TLR ligand, IL-12p70 production is observed, which polarizes the T-cells to Th1 effector cells. $CD11b^+$ DCs on the other hand, produce inflammatory chemokines such as CCL3, CCL4 and CCL5 upon TLR-stimulation with lipopolysaccharide (LPS), polyinosinic-polycytidylic acid (PolyIC) and oligodeoxynucleotides with a CpG motif (CpG) (25, 26). Furthermore, the peripheral equivalents of $CD8\alpha^+$ DCs are $CD1O3^+$ DCs, characterized by the same functions although performed in the periphery instead of lymphoid organs.

1.1.2 Plasmacytoid dendritic cells (pDCs)

pDCs represent a DC subset specialized in the production of type I interferons (IFN-I) in response to the exposure to viruses or virus-infected cells (27). This process occurs *via* two PRRs that reside within the endosomal compartments: TLR-7 and TLR-9. By secreting different cytokines, particularly IFN-I but also IL-12 and IL-6, pDCs regulate various types of immune responses. IFN-I secretion by pDCs not only activates natural killer (NK) cell cytotoxicity, but in combination with IL-12, pDCs induce IFNγ-secreting NK cells, $CD8^+$ and $CD4^+$ T-cells, thus aiding in the clearance of intracellular pathogens (28). Additionally, when

IL-6 is secreted in combination with IFN-I, pDCs induce differentiation of B-cells into plasma cells, promoting the production of anti-viral antibodies (28, 29). Apart from cytokine secretion, activated pDCs change phenotypically as they acquire a dendritic morphology and up-regulate MHC and co-stimulatory molecules. This process enables pDCs to direct T-cell responses *via* antigen presentation resulting in their proliferation, albeit in a lower extent compared to cDCs. This latter can be explained by the lower expression of MHC and co-stimulatory molecules than their cDC counterparts (28, 30). Additional to their role in inducing immunogenic responses, pDCs have shown to be able to induce Treg cells resulting in T-cell tolerance (30, 31). In steady state, pDCs are found in the thymus, spleen and lymph nodes, but also in most peripheral tissues in lower frequencies (32).

1.1.3 Monocyte-derived dendritic cells (inflammatory DCs, iDCs)

As the name suggests, this type of DCs is derived from monocytes in the context of inflammation but also, although less efficiently, in steady state. There are two subpopulations of monocytes *i.e.* $LyC6^{high}$ and $LyC6^{low}$ monocytes. The $LyC6^{high}$ monocytes are also referred to as "inflammatory" monocytes, as they migrate robustly to sites of inflammation. This in contrary to $LyC6^{low}$ monocytes, which monitor the blood stream and travel into peripheral tissues in steady state, provoking their designation as "resident" monocytes. Additionally, this subgroup of monocytes seems to be involved in the reconstitution of tissue macrophages and DCs (33). Inflammatory monocytes respond to inflammation by massively migrating from the bone marrow to the inflamed site where they differentiate into inflammatory DCs (iDCs). This differentiation is characterized by the up-regulation of MHC II antigens, CD11c and co-stimulatory molecules such as CD40, CD80 and CD86 and is controlled by the granulocyte-monocyte colony-stimulating factor (GM-CSF) (34). Following their differentiation into iDCs locally, they migrate to the draining lymph nodes where antigen-specific T-cell proliferation is stimulated. In addition to activation of $CD4^{+}$ T-cell responses, they can also cross-present antigens to $CD8^{+}$ T-cells and coordinate the production of immunoglobulins by B-cells. Furthermore, iDCs produce tumor necrosis factor (TNF) and inducible nitric oxide synthetase (iNOS) in response to microbial exposure, giving rise to their microbicidal potential (35). In this context it was demonstrated that chemokines (C-C motif) receptor 2 (CCR2) deficient mice, which are no longer able to recruit monocytes to the site of infection, are highly susceptible to *Listeria monocytogenes* infection and die within four days, emphasizing the significance of iDCs in pathogen immunity (33, 36, 37). Collectively, these DCs are important players in both innate and adaptive immunity.

Mouse bone marrow cultures in the presence of GM-CSF give rise to iDCs, making it possible to generate this type of DCs *in vitro* (18). In addition, mouse DCs can also be obtained *in vitro* from bone marrow cultures in the presence of the growth factor fms-like tyrosine kinase 3 ligand (Flt3L). In this culture, other DC subsets will be produced, such as pDCs and cDCs (38).

1.1.4 Migratory DCs

As the lymph node (LN)-resident DCs do not leave the LNs, they must gain access to tissue-derived antigens in a different way. Antigens could directly access LN-resident DCs via the lymph vessels, although this leads to relatively ineffective T-cell responses (39). Alternatively, migratory DCs act as antigen-collectors in the periphery and upon migration to the regional lymph nodes, they either present the antigen themselves to the T-cells or they transfer the antigen to lymph node-resident DCs (39). Migratory DCs can therefore be found in all peripheral tissues including the liver, dermis, lung, kidneys and intestinal tract, but also in the lymph nodes. They can be divided in CD11b$^+$ and CD103$^+$ DCs, which represent the peripheral equivalents for CD11b$^+$ and CD8α^+ lymphoid-resident DCs respectively. Comparable to their lymphoid-resident counterparts, CD11b$^+$ migratory DCs present their acquired antigens more efficiently to CD4$^+$ T-cells, whereas CD103$^+$ migratory DCs preferably cross-present extracellular antigens to CD8$^+$ T-cells (40).

1.1.5 Langerhans cells (LCs)

Langerhans cells are DCs present in the epidermis that constantly monitor the environment for invading pathogens (41). More information about this type of DCs is described in literature but is not covered within the scope of this thesis.

As described above, DCs become activated upon PRR-stimulation and initiate maturation to eventually present antigens to naïve T cells. Interestingly, recent studies have demonstrated an additional pathway that contributes to DC activation. More specifically, ER stress was proven to be induced in DCs upon pathogen or damage detection, which can be explained by the ability of DCs to process the engulfed antigens to peptides. This processing requires high enzymatic capacity and "plunders" the cellular machinery of the DCs, which ultimately leads to the accumulation of unfolded proteins in the endoplasmic reticulum (ER) and this way induces ER stress (42).

1.2 Endoplasmic reticulum stress

The ER is a multi-functional organelle found in cells of all eukaryotic organisms. Not only it is responsible for the proper folding of newly synthesized secreted and membrane-bound proteins, but it also serves as an important calcium reservoir (43). These two functions are interdependent as a constant luminal calcium concentration is necessary for correct protein folding and vice versa. The oxidative environment of the ER promotes protein folding and facilitates disulfide bond formation and additional post-translational modifications (43). Importantly, protein folding is constantly monitored and supported by ER-resident chaperones and folding enzymes, such as calnexin and immunoglobulin-heavy-chain-binding protein (BiP) in a process called ER quality control (44). This process ensures that only properly folded proteins can exit the ER. Therefore, if proteins are misfolded, they are retained at the ER until they reach an appropriate conformation or, if the damage is too severe, they are sent for degradation through a process called ER-associated protein degradation (ERAD) (45). However, when the protein folding capacity of the ER is compromised, such as by an increase in folding demand or by reduced enzymatic capacity, unfolded proteins accumulate in the ER. This process leads to ER stress, which triggers the activation of a signaling pathway, the UPR (46). There are many types of insults that trigger ER stress including hypoxia, calcium depletion and glucose deprivation (47). The UPR subsequently transfers this information from the ER to the nucleus and cytoplasm, where transcriptional and translational processes are adjusted to the current protein folding state. Not only is this signaling pathway responsible for a reduced input of nascent polypeptides and degradation of misfolded ones, but it also coordinates the transcriptional up-regulation of ER chaperones and folding enzymes (48, 49). These events function to ultimately alleviate ER stress, by reducing the biosynthetic load and stimulating the folding capacity of the ER respectively. Nevertheless, when accumulation of unfolded proteins is sustained and the stress becomes too severe, the UPR will not be sufficient to regain homeostasis and proteins will undergo apoptosis (46, 48).

Inositol-requiring protein-1 (IRE1), protein kinase-like ER kinase (PERK) and activating transcription factor 6 (ATF6) are the three main sensors of ER stress (figure 3). Activation of these proteins occurs *via* interaction with BiP, which, in absence of ER stress, binds to and inhibits these sensors. When unfolded proteins accumulate in the ER, the pool of free BiP decreases as this chaperone is trapped by the increased amount of unfolded proteins. This leads to the release of BiP from the sensors, followed by their activation and the initiation of signaling cascades (50).
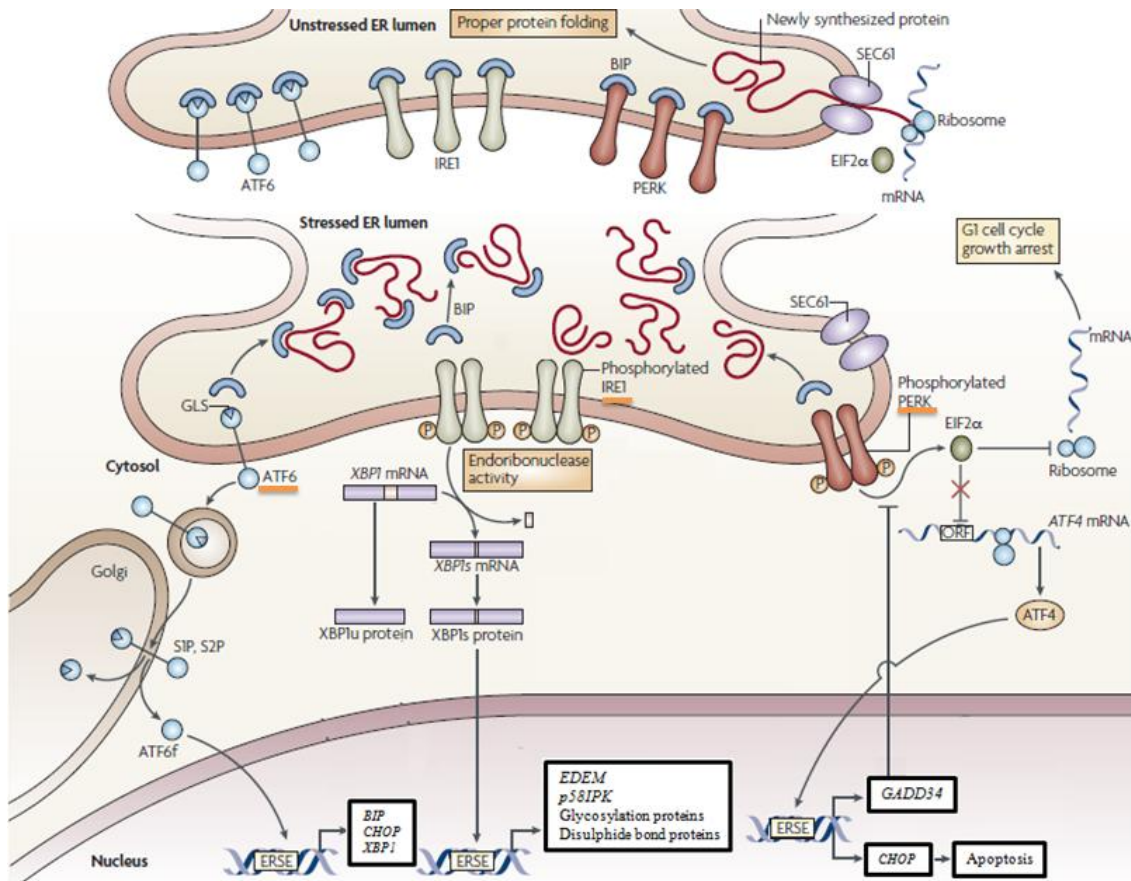
Figure 3: The unfolded protein response. In the absence of ER stress, immunoglobulin-heavy-chain-binding protein (BiP) binds to and inhibits the three main sensors of ER stress, inositol-requiring protein-1 (IRE1), protein kinase-like ER kinase (PERK) and activating transcription factor 6 (ATF6). When unfolded proteins accumulate in the ER lumen, BiP is released from the sensors, which leads to their activation and initiation of three events: 1) ATF6 is cleaved by two proteases, site-1 (S1P) and site-2 protease (S2P), releasing the transcription factor domain (ATF6f). This fragment subsequently transfers to the nucleus, binds to ER stress responsive elements (ERSEs) and activates the transcription of unfolded protein response (UPR) target genes. 2) IRE1 undergoes dimerization and autophosphorylation, leading to the activation of its endoribonuclease domain. This domain excises 26 nucleotides from *Xbp1* mRNA, resulting in the conversion from the unspliced form of *Xbp1* (*Xbp1u*) to a mature, spliced form of *Xbp1* (*Xbp1s*). XBP1s functions as a transcription factor, inducing transcription of several ER stress-related genes. 3) PERK also undergoes dimerization and autophosphorylation upon activation, resulting in the phosphorylation of the α subunit of eukaryotic initiation factor 2 (eIF2α). This inactivates eIF2 leading to the inhibition of protein translation. Additionally, translation of some mRNAs is promoted upon inactivation of eIF2, such as *Atf4*. Adapted from Todd *et al.* (51).

1.2.1   ATF6

ATF6 is a transmembrane protein comprised of a C-terminal ER stress sensing domain oriented to the ER lumen and an N-terminal transcription factor domain oriented to the cytosol. Upon ER stress and thus release from BiP, ATF6 translocates to the Golgi complex

where it encounters two proteases, site-1 (S1P) and site-2 protease (S2P) that are able to release the transcription factor domain. This domain subsequently transfers to the nucleus where it binds to and activates transcription of conserved ER stress responsive elements (ERSEs). These elements are present in multiple copies in the promoters of UPR target genes such as ER chaperones and folding enzymes (50, 52). Interestingly, XBP1 also appeared to be a target gene of ATF-6, creating a link with the IRE1 pathway which is discussed below (53).

1.2.2 PERK

The second molecule that is activated by the accumulation of unfolded proteins in the ER is PERK. This protein kinase undergoes dimerization and autophosphorylation, leading to a conformational change so that PERK is now able to recognize and phosphorylate the α subunit of eukaryotic initiation factor 2 (eIF2α). Once eIF2α is phosphorylated, eIF2 is inactivated, leading to the attenuation of protein translation by inhibiting the delivery of the methionyl-tRNA to the ribosome (50, 54). Remarkably, translation of some mRNAs is promoted when eIF2 activity is decreased. These mRNAs contain short upstream open reading frames and *Atf4* is the most representative one. This latter gene is responsible for the activation of C/EBP homologous protein (CHOP) and growth arrest and DNA damage-inducible 34 (GADD34). CHOP is a transcription factor involved in the stimulation of apoptosis, thus providing a mechanism of cell death in conditions of prolonged stress. GADD34 on the other hand, provides recovery from translational attenuation *via* recruitment of protein phosphatase 1 that dephosphorylates eIF2α (52).

1.2.3 IRE1

IRE1 is a bifunctional transmembrane protein consisting of a dimerization domain oriented to the ER lumen and both a serine/threonine kinase and endoribonuclease domain oriented to the cytosol. Upon activation, IRE1 undergoes dimerization and autophosphorylation, leading to the activation of its endoribonuclease domain. This latter recognizes the mRNA encoding the X-box binding protein 1 (XBP1) and excises 26 nucleotides, resulting in a shift in the codon reading frame after ligation of the detached exons (55). This shift in translation generates an alternative COOH-terminal that contains an additional potent transactivation domain. Translation of the new reading frame leads to the conversion of unspliced XBP1 (XBP1$_U$) to a mature, spliced form of XBP1 (XBP1$_S$) which functions as a transcription factor (56). In this manner, transcription of ER stress-related genes is controlled, such as those involved in

protein folding, ERAD, quality control and protein entry and transport to and from the ER respectively (57).

XBP1$_S$ is required for the differentiation of B cells in antibody-secreting plasma cells and for the development and function of highly secretory cells such as pancreatic, salivary gland and intestinal epithelial cells. In these cells, XBP1$_S$ induces expansion of the ER, organelle biogenesis and total protein synthesis, all of which are vital characteristics for secretory cells (52, 58-60).

Activation of the IRE1 pathway is an evolutionarily conserved feature and cells in homeostasis (with the exception of highly secretory cells and plasma cells) do not significantly activate the pathway (51). However, experiments using XBP1 RAG-2$^{-/-}$ mice demonstrated that this type of mice is characterized by reduced numbers of cDCs and pDCs, with pDCs being the most affected subset. They also showed constitutive activation of the IRE1-XBP1 pathway, as indicated by the high level of XBP1$_S$ in the DCs. Again, this was more abundant in the pDC subset, which is not surprising since pDCs secrete high levels of IFN-1 upon viral activation for which a highly elaborate ER is required. Together, it seems that a basal XBP1 activation is necessary for optimal DC survival, development and function, probably due to their enormous capacity to process proteins and secrete cytokines (61).

Additionally, it was recently reported that not only inflammation may contribute to the induction of ER stress (62), but inversely, ER stress can enhance inflammation too. This is thought to occur among others *via* IRE1-mediated NF-κB activation, which plays an essential role in the regulation of the immune response (63, 64).

Hu *et al.* demonstrated that ER stress and XBP1 in particular, synergizes with polyIC-induced production of IFN-β and inflammatory cytokines in murine DCs (65). PolyIC is a synthetic mimic of viral dsRNA used in cultures that is able to activate DCs *in vitro* by binding to the PRRs TLR-3 and MDA-5. As described above, DCs are equipped with various PRRs that render them capable to react to different PAMPs/DAMPs. Additionally, PRRs are heterogeneously distributed among different DC subsets, resulting in distinct responses when ligated by different microbial molecules. This was also observed in the experiments of Hu *et al.*, where XBP1 activation of iDCs did not promote IFN-β production upon stimulation with ssRNA, a TLR-7 agonist, or CpG, a TLR-9 agonist instead of polyIC. pDCs, on the other hand, did show higher cytokine production in these circumstances, pointing towards their higher levels of TLR-7 and TLR-9 compared to iDCs (65). This heterogeneous distribution makes it highly interesting to investigate the influence of ER stress on each subset.

Apart from DCs, Martinon *et al.* (62) demonstrated an interconnection between innate immunity and the IRE1-XBP1 signaling pathway in macrophages. Remarkably, the XBP1 signaling pathway became activated upon TLR-engagement of macrophages without inducing ER-stress target genes of XBP1 or other ER-stress related genes or, such as *Erdj4, Bip, Atf6, Perk* and *Chop*. Instead, XBP1-activation functioned to support enhanced and sustained production of pro-inflammatory mediators such as IL-6, TNF and IFN-β in these immune cells, providing a link with the innate immune system (62). The relevance of this positive link between the UPR and the innate immune system was provided directly since mice that were deficient in XBP1 experienced a much greater bacterial burden upon infection with *Francisella tularensis* (a TLR2-binding pathogen).

Since abnormalities of the ER stress pathway and innate immunity lie at the roots of many diverse diseases (66), improved insight in the cross-link between these two pathways may provide a first step towards novel therapies and enhanced comprehension of the pathogenesis of these diseases.

1.3   Question

This project aims at identifying the role of XBP1 in iDC survival, activation and the regulation of its functions.

1. Our first objective was to determine the potential cross-link between PRR-signaling and the UPR in iDCs.

2. Our second objective was to characterize the role of iDC survival, maturation and function.

3. Our last objective was to investigate the effect of XBP1 deficiency on ER stress management in these DCs.

2   <u>Materials and methods</u>

Table I: Used media, buffers and reagentia:

RBC lysis -buffer	0.15 M NH_4Cl, 1 mM $KHCO_3$, 0.1 mM Na_2EDTA in milliQ H_2O
TCM	RPMI-1640, 5 % FCS, 2.8 ml 0.05 mg/ml gentamycine, 0.5 ml50 µM β-mercaptoethanol
Washing buffer ELISA	PBS, 0.05% Tween-20 (Sigma)
FACS buffer	PBS, 0.25 % BSA, 0.5 mM EDTA, 0.05 % NaN_3

E1A lysis buffer	250 mM NaCl, 20 mM HEPES (pH 7.9), 1% NP-40, 1 mM EDTA, protease inhibitor kit (Complete and PhosStop, Roche)
Laemmli buffer (4x)	3.8 ml ddH$_2$O, 1ml Tris-HCL 0.5M, pH 6.8, 0.8 ml glycerol, 1.6 ml SDS 10%, 0.4 ml 2-mercaptoethanol, 0.4 ml 1% w/v bromophenol blue
Running-Transfer buffer (5x)	60 g Tris Base, 288 g Glycine, 4 l ddH$_2$O
Run Tris-SDS	90.85 g 1.5 M Tris, 2 g 0.4% SDS, 500 ml ddH$_2$O
Stack Tris-SDS	30.28 g 0.5 M Tris, 2 g 0.4% SDS, 500 ml ddH$_2$O
Acrylamide 30%	146 g acrylamide, 4 g N'N'-bis-methyl-acrylamide, 500 ml ddH$_2$O
APS 10%	1g ammonium persulfate, 10 ml ddH$_2$O
Migration buffer	200 ml 5x Running-Transfer Buffer, 10 ml SDS 10%, 790 ml ddH$_2$O
Transfer buffer	100 ml 5x Running-Transfer buffer, 100 ml methanol, 300 ml ddH$_2$O
Ponceau Red	0.2 g Ponceau S, 3 g trichloroacetic acid, 3 g sulfosalycic acid, 100 ml ddH$_2$O
TBS (10x)	80 g NaCl, 24.2 g Tris-Base, 1 l H$_2$0, pH 7.6

RBC, red blood cell; EDTA, ethylenediaminetetraacetic acid ; TCM, tissue culture medium; RPMI, Roswell Park Memorial Institute; FCS, fetal calf serum; PBS, phosphate buffered saline; BSA, bovine serum albumin; HEPES, (4-(2-hydroxyethyl)-1-piperazineethanesulfonic acid; SDS, Sodium dodecyl sulfate; APS, ammonium persulfate.

2.1 Mice

For this research CD11c Cre$^{+/-}$ mice were used of which exon 2 of *Xbp1* is flanked by two loxP-sites (XBP1$^{fl/fl}$). This Cre-loxP system is a technique to generate a tissue- or cell-specific deletion of a certain gene (figure 4). In these mice, expression of the Cre-recombinase is controlled by the CD11c promoter, which is mostly specific for DCs and results in the excision of exon 2 of *Xbp1*. On its turn, this creates a frame shift making *Xbp1* no longer functional.

Initially, homozygous XBP1$^{fl/fl}$ mice are crossed with CD11c Cre mice that are equipped with two wild type XBP1 alleles (CD11c Cre$^+$ XBP1$^{wt/wt}$). 50% of the F1 off-springs are heterozygous and express the Cre-recombinase under control of the CD11c promoter (CD11c Cre$^+$ XBP1$^{fl/wt}$). By interbreeding these CD11c Cre$^+$ XBP1$^{fl/wt}$ mice with homozygous

XBP1$^{fl/fl}$ mice, homozygous CD11c Cre$^+$ XBP1$^{fl/fl}$ mice can be obtained. At the age of 6 to 10 weeks, the mice were sacrificed with carbon dioxide (CO_2) to collect bone marrow.
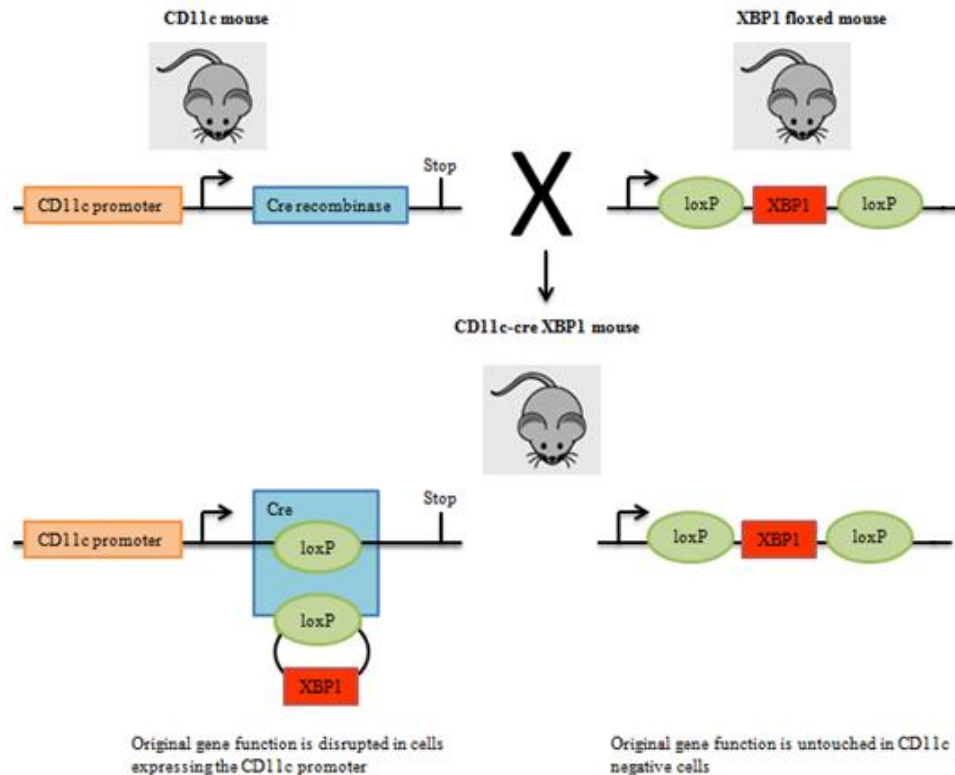

Figure 4: The Cre-LoxP system. By crossing a homozygous mouse that contains the Cre-recombinase downstream of the CD11c promoter (CD11c Cre$^+$ XBP1$^{wt/wt}$) with a homozygous mouse containing *Xbp1* in which two loxP sites are inserted (CD11c Cre$^-$ XBP1$^{fl/fl}$), 50% of the F1 off-springs are heterozygous and express the Cre-recombinase (CD11c Cre$^+$ XBP1$^{fl/wt}$) (not represented on the figure). Interbreeding of these heterozygous F1 off-springs with homozygous XBP$^{fl/fl}$ mice results in the birth of homozygous CD11c Cre$^+$ XBP1$^{fl/fl}$ mice. These mice will only express *Xbp1* in CD11c negative cells.

2.2 Culture of bone marrow-derived DCs

For the culture of bone marrow-derived DCs (BMDCs), the limbs from the mice were isolated. The bones were then collected in cold Hanks' Balanced Salt Solution (HBSS, Gibco) and incubated shortly with 70% ethanol (Merck) for sterilization. Subsequently, the bones were cut at the ends and flushed with HBSS. The cells were filtered through a nylon cell strainer into a 50 ml tube and spun down (400 x *g*, 7 min, 4°C). The cells were then resuspended in red blood cell (RBC) lysis-buffer (1 + # mice x 1 ml = # ml RBC lysis-buffer) (Table I) and incubated for 2 minutes at room temperature (RT). Excess ice-cold HBSS was added to inactivate the lysis and the cells were spun again. The cell pellet was resuspended in 10 ml tissue culture medium (TCM) (Table I) and cells were counted (1:10) with trypan blue (Fluca). To make a culture, the cells were put in 100 mm culture dishes at a concentration of

2-3 x 10^6 cells in 10 ml TCM with 20 ng/ml GM-CSF (recombinant mouse GM-CSF, received from Kris Thielemans, VUB). At day 3 of the culture, we added 10 ml of fresh TCM with 20 ng/ml GM-CSF to the plates. At day 6 we replaced 10 ml of medium with fresh TCM together with 20 ng/ml GM-CSF per plate and put it back in the original plates. After 8 days of culture, the cells were harvested by collecting the supernatant of the plates in 50 ml tubes. To gain as much cells as possible, the plates were rinsed with a small amount of phosphate buffered saline (PBS) after which this was also added to the 50 ml tubes and these were centrifuged (400 x g, 7 min, 4°C). The cell pellet was resuspended in 5 ml TCM and cells were counted (1:10) with trypan blue to determine the final yield of the bone marrow culture.

2.3   Quantitative real-time polymerase chain reaction

To assess the effect of *Xbp1* deletion on the function of BMDCs, the secretion of different cytokines upon stimulation was measured by quantitative real-time polymerase chain reaction (qrt-PCR) and compared to wild type (WT) DCs. This technique was also used to check to what degree distinct PRR-stimuli are able to trigger ER stress. For this purpose the induction of ER stress genes (*Bip, Edem, Sec61, Xbp1*) after stimulation was measured.

2.3.1   RNA isolation

The RNA isolation was performed with Tripure Isolation Reagent (Roche)

2.3.1.1   Stimulation of BMDCs

Before RNA-isolation from the *in vitro* generated BMDCs, the DCs were stimulated with different conditions represented in table II or were untreated as a negative control, to obtain maturation.

Table II: Different stimuli

Stimuli	Stock concentration	Final concentration	Target
Tunicamycin (Sigma)	10 mg/ml	2 µg/ml	Inducer of ER stress
LPS (InvivoGen)	100 µg/ml	200 ng/ml	TLR4
HDM (Greer)	5 mg/ml	100 µg/ml	TLR4, Dectin-2
CpG (Invivogen)	1 mg/ml	2 µg/ml	TLR9
Cdl (Wako)	10 mg/ml	200 µg/ml	Dectin-1
PolyIC (Sigma)	5 mg/ml	100 µg/ml	MDA-5, TLR3

LPS, lipopolysaccharide; HDM, house dust mite; Cdl, curdlan; TLR, toll-like receptor; MDA-5, melanoma differentiation-associated protein 5.

For this purpose, 5 x 10^5 cells were plated per well in 24-well plates and stimulated. Subsequently RNA was with1 ml Tripure Isolation Reagent per condition.

2.3.1.2 Phase separation

The next step is to add 200 µl chloroform (Sigma-Aldrich) to the tubes, followed by inverting the tubes for 30 seconds. After 15 minutes of incubation at RT, the tubes were spun down (12000 x *g*, 15 min, 4°C) and the aqueous phase, which contains the RNA, was transferred to fresh eppendorphs.

2.3.1.3 RNA precipitation

To precipitate the RNA, 500 µl isopropanol (Merck) was added together with 0.5 µl glycogen, an inert co-precipitant of nucleic acids which increases the yield of RNA. Upon 15 minutes of incubation at RT, the tubes were centrifuged again (12000 x *g*, 10 min, 4°C).

2.3.1.4 RNA rinsing

After removal of the supernatant, the pellet was washed with 1 ml 75% ethanol and the tubes were spun (7500 x *g*, 5 min, 4°C).

2.3.1.5 Dissolving the RNA

Subsequent to discarding the supernatant, the pellet was dried on air for 15-30 minutes and dissolved in 20 µl PCR-grade water (Roche). The tubes were incubated for 10 minutes at 55°C and kept on ice from then on. To assess the purity and concentration of the RNA, analysis with Nanodrop (ND-8000) was performed. Finally, the RNA was frozen at -20°C.

2.3.2 cDNA synthesis

cDNA synthesis was performed with the Transcripton High Fidelity cDNA Synthesis Kit (Roche). In a first step, the template-primer mix was made for each sample by adding the components represented in table III to an RNase-free PCR tube.

Table III: Components for the template-primer mix (for one reaction)

Component	Volume	Final concentration
Total RNA	Variable	500 ng
Random Hexamer primer	2 µl	60 µM
Water, PCR-grade	Variable	--
Final volume	**11.4 µl**	

The PCR tube was heated for 10 minutes at 65°C, leading to the denaturation of the template-primer mix. Next, the tube was cooled at 4°C and the remaining components of the reverse transcriptase mix were added to the tubes (Table IV) to finally have 20 µl.

Table IV: Remaining components for the reverse transcriptase mix (for one reaction)

Component	Volume	Final concentration
Transcriptor High Fidelity Reverse Transcriptase Reaction Buffer (5x)	4 µl	1x
Protector RNase Inhibitor	0.5 µl	20 U
Deoxynucleotide Mix	2 µl	1 mM each
DTT	1 µl	5 mM
Transcriptor High Fidelity Reverse Transcriptase	1.1 µl	10 U
Final volume	**20 µl**	

Upon addition, the reaction was incubated for 10 minutes at 29°C and 60 minutes at 48°C. Subsequently, it was heated at 85°C for 5 minutes to inactivate the reverse transcriptase. Finally, the cDNA was diluted 1:5 or more with PCR-grade water and was storaged at -20°C.

2.3.3   qrt-PCR

With qrt-PCR, mRNA expression of *Xbp1* (exon 2, for genotyping), different cytokines (*Il6, Il12 and Tnf*) and ER stress genes (*Bip, Edem and Sec61*) was evaluated relative to the expression of the housekeeping gene *L27*. For this end, the Lightcycler 480 Probes Master Kit (Roche) was used. Amplification of the cDNA was implemented with primers that recognize specific sequences (table V). To start, the PCR mix for every primer couple was prepared by adding the components in table VI to a 1.5 ml tube.

Table V: Used primer sequences for qrt-PCR

Gene	Forward primer	Reverse primer
Xbp1(62)	CAGCAAGTGGTGGATTTGG	CGTGAGTTTTCTCCCGTAAAAG
Il6	ACACATGTTCTCTGGGAAATCGT	AAGTGCATCATCGTTGTTCATACA
Il12	ACTCTGCGCCAGAAACCTC	CACCCTGTTGATGGTCACGAC
Tnf	CTGTAGCCCACGTCGTAGC	TTGAGATCCATGCCGTTG
Bip	ATGAGGCTGTAGCCTATGGG	GGGGACAAACATCAAGCAG
Edem (67)	AAGCCCTCTGGAACTTGCG	AACCCAATGGCCTGTCTGG

Sec61 (67)	CTATTTCCAGGGCTTCCGAGT	AGGTGTTGTACTGGCCTCGGT

XBP1, X-box binding protein 1; IL, interleukin; TNF, tumor necrosis factor; BiP, immunoglobulin-heavy-chain-binding protein; EDEM, ER degradation-enhancing α mannosidase-like protein.

Table VI: qrt-PCR mix for one reaction

Component	Volume
SYBR Green Master Mix	7.5 µl
PCR primers (forward and reverse)	0.375 µl
Final volume	**7.875 µl**

The mix was vortexed and 7.875 µl was added to each well of the Lightcycler 480 multiwell plate, together with 7.125 µl of cDNA. Upon sealing the plate with foil, it was centrifuged at 400 x g, for 5 seconds and transferred into the LightCycler 480 Instrument. A non-template control (PCR-grade water) was included for each primer set to detect non-specific amplification. The applied qrt-PCR program is described in table VII.

Table VII: Quantitative real-time PCR reaction

Step	Cycles	Temperature (°C)	Time
Dissociation	1	95	5'
Amplification			
Dissociation		95	10''
Annealing	45	60	10''
Elongation		72	20''
Cooling	1	40	30''

2.4 Agarose Gel electrophoresis

An agarose gel electrophoresis was performed to assess the splicing of *Xbp1* (table II). For this purpose, the sequence of *Xbp1* was first amplified with primers by PCR to gain enough material for analysis. The primers that were used specifically recognized *Xbp1* sequences that encompass the splicing regions recognized by *Ire1* (5′-ACACGCTTGGGAATGGACAC-3′ and 5′-CCATGGGAAGATGTTCTGGG-3′). This makes it possible to detect both the spliced and unspliced form of XBP1 (62).

2.4.1 PCR

For this experiment, the Taq DNA Polymerase Kit (Roche) was used. Initially, a Master Mix was prepared that contained all reaction components represented in table VIII.

Table VIII: PCR mix for one reaction

Component	Volume	Final concentration
PCR Grade Nucleotide Mix (10 mM of each dNTP)	1 µl	200 µM (of each dNTP)
Primers (Forward + Reverse)	1 µl	0.2 µM
Water, PCR grade	37.2 µl	--
PCR reaction buffer, 10×	5 µl	1× (1.5 mM MgCl2)
Taq DNA Polymerase (5 U/µl)	0.8 µl	0.89 U/µl
Final volume	**45 µl**	

To produce a homogeneous reaction, the mix was vortexed gently before adding 45 µl to each well of a PCR 96 well-plate. Subsequently, 5µl of the cDNA was pipetted to every well and the plate was sealed with foil before loading into the PCR thermal block cycler. The PCR protocol is described in table IX.

Table IX: PCR reaction

Step	Cycles	Temperature (°C)	Time
Initial denaturation	1	95	8'
Denaturation	35	95	30''
Annealing		60	30''
Elongation		72	30''
Final elongation	1	72	10'
Cooling	1	4	Indefinitely

2.4.2 Agarose gel electrophoresis

After cycling, agarose gel electrophoresis was done to separate DNA fragments according to their size by applying an electric field. The agarose gel functions as a matrix in which smaller fragments migrate faster than larger ones, $Xbp1_U$ (171 bp) will therefore have a slower migration rate than the spliced form (145 bp). Since the difference between the two DNA

fragments is only 26 bp, a 2.5% agarose gel (2.5g Agarose MS (Roche), 100ml TBE buffer 1X (Roche) was used to allow a good resolution and the PCR products were visualized by DNA Stain G (Serva). Before loading the samples on the gel, 1x loading buffer was added to the samples to increase the sample density and allow visualization of the migration. By adding a molecular weight marker XIV (100 bp ladder) (Roche) to the gel, the size of the DNA fragments could be determined. Finally, the gel was run at 100 V for 30 minutes and was viewed on a UV transiluminator to capture a photographic image.

2.5   ELISA (eBioscience)

Cytokine production was also analyzed with Enzyme-Linked Immuno Sorbent Assay (ELISA), an immunochemical technique based on the specific binding of an antibody with its antigen (Figure 5).
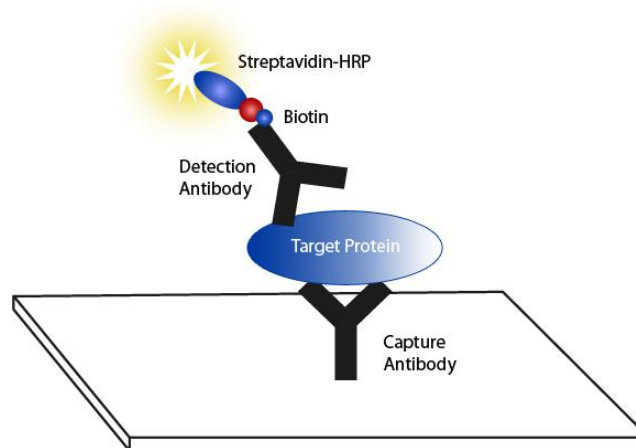

Figure 5: Principle of ELISA. The target protein is bound by capture antibodies and detection antibodies. The latter are conjugated to biotin, which binds to streptavidin coupled to horseradish peroxidase (HRP). This provides a colorimetric signal, which allows visualization of the target protein. Adapted from Hornbeck *et al.* (68)

The ready-set-go kit from eBioscience was used and flat-bottom 96 half area well plates (Greiner) were coated with 50 µl capture antibodies (anti-mouse monoclonal Ab, eBioscience, table X) in the right dilution with coating buffer (eBioscience) and incubated overnight at 4°C.

Table X: ELISA information

Cytokine	Dilution capture Ab (stock conc.)	Dilution supernatant (stock conc.)	Dilution detection Ab	Conc. highest standard	Dilution Streptavidin-HRP
IL-6	1/250	1/100	1/250	500 pg/ml	1/250
IL-10	1/1000	Undiluted	1/1000	4000 pg/ml	1/250
IL-12	1/250	Undiluted	1/250	2000 pg/ml	1/250
TNF	1/250	1/50	1/250	1000 pg/ml	1/250

IL, interleukin; TNF, tumor necrosis factor.

The next morning, the wells were washed 5 times with washing buffer (Table I) and 150 µl blocking buffer (1x Assay Diluent, eBioscience) was added to each well, followed by incubation for 1 hour at RT. Subsequently, the wells were washed 3 times and our samples of the culture supernatants, the standards (1/2 serial dilution) and a blank was added. Appropriate dilutions of the samples and standards (eBioscience) were obtained with assay diluents (table X) and each sample was added in triplicate.

After an incubation of 2 hours at RT, the plates were washed 5 times and 50 µl detection antibody (eBioscience) was added (Table X) followed by another incubation of 1 hour at RT. The plates were washed 5 times and 50 µl streptavidin-HRP (eBioscience) (diluted in Assay Diluent, table X) was added. After 30 minutes of incubation at RT, the plates were washed 7 times and 50 µl of substrate solution was added to each well (equal volumes of peroxidase solution B and TMB peroxidase substrate, eBioscience). Then the wells were incubated in the dark until the highest concentrations of the standard clearly became blue, but the blanks did not. To stop the reaction, 25 µl stop solution (2N H_2SO_4, Fluka) was added to each well and finally the absorbance was read at 450 nm with Victor³ (PerkinElmer, 1420 Multilabel Counter). The concentration of cytokines could be calculated with the calibration curve obtained from the standards.

2.6 Flow cytometry

To evaluate the potential role of XBP1 in DC maturation, expression of co-stimulatory molecules (CD40 and CD86) and CD11c was measured by flow cytometry. DC survival was also assessed with flow cytometry, by determining the percentage of alive CD11c$^+$ DCs in the non-debris gate. The cells were resuspended in 100 µl FACS-buffer (Table I) and transferred to a 96-well plate before centrifuging (400 x g, 3 min, 4°C). Upon aspiration of the

supernatant, 50 µl of the antibody mix was added. This mix contained fluorochrome-labeled antibodies that we were interested in, diluted in FACS-buffer (table XI).

Table XI: Fluorochrome-labeled antibodies and their dilutions used for flow cytometry of BMDCs

Antigen	Clone	Fluorochrome	Dilution
CD11c (Invitrogen)	N418	PE-Texas Red	1/150
CD86 (Biolegend)	PO3	PE-Cy7	1/100
CD40 (BD)	'3/23	APC	1/50
Live/dead marker (Invitrogen)		Amcyan	1/200 (diluted in PBS)

After resuspending the samples in this mix and preparation of single staining controls, the 96-well plate was incubated for 30 minutes at 4°C. Subsequently, 150 µl PBS was added to each well and the plate was centrifuged (400 x g, 3 min, 4°C). Upon aspiration of the supernatant, the samples were resuspended in 50 µl Amcyan (1/200 in PBS), which was used as a live/dead marker followed by 15 minutes of incubation at RT in the dark. 150 µl of PBS was added again and the plate was centrifuged (400 x g, 3 min, 4°C). Finally, the pellets were resuspended in 100 µl of PBS and transferred to FACS tubes, ready to be measured with the flow cytometer (BD LSRII). The results were analyzed with FlowJo.

2.7 Western Blot

To correlate the gene expression level of ER stress genes with the protein expression level, a Western Blot analysis was performed. The purpose of this experiment is to separate proteins on a gel according to their molecular weight and transfer these proteins to a membrane for identification by an antibody-linked enzymatic reaction.

Briefly, the BMDCs were plated at 1 x 10^6/well in a 24-well plate and stimulated with the conditions represented in table II. After 8 hours of stimulation, proteins were extracted by scraping the bottom of the wells in order to detach as much cells as possible. 1 ml of the suspension was transferred to eppendorphs and these were centrifuged (400 x g, 7 min, 4°C). After aspiration of the supernatant, 1 ml of cold PBS was added and the tubes were spun again (400 x g, 7 min, 4°C). Again, the supernatant was aspirated and the remaining pellet was finally resuspended in 20 µl E1A lysis buffer (Table I). Since the samples could not be

used immediately, they were frozen at -20°C. Later, the protein lysates were thawed, spun down (13000 RPM, 10 min, 4°C) and the supernatant was transferred to new tubes.

2.7.1 Biorad Bradford Protein Assay

Protein concentration was determined with a Biorad Bradford Protein Assay. For the standards, dilutions of bovine serum albumin (BSA, New England Biolabs) were made in pure water starting at 0 µg/ml and ending with 200 µg/ml (table XII) in an ELISA plate (flat bottom). The BSA dilutions were subsequently diluted again (1/5) with Bradford (5x, Bio-Rad), providing a colorimetric signal. The samples were first diluted 1/100 with pure water and then 1/5 with Bradford. Finally the absorbance was measured at 595 nm.

Table XII: Dilutions of BSA

BSA (in kµl)	0	20	40	60	80	100	120	140	160	180	200
H_2O (in µl)	200	180	160	140	120	100	80	60	40	20	0
Final conc. BSA (in µg/ml)	0	10	20	30	40	50	60	70	80	90	100

2.7.2 Western Blot

The protein extracts were mixed with 1x Laemmli buffer (Table I) and heated for 5 minutes at 95°C. Before blotting, an 8% acrylamide gel was prepared since we were interested in XBP1 and BiP, proteins of 55 and 78 kDa respectively. This gel is composed of two parts, a stacking gel to concentrate the proteins before separating and a running gel for the actual separation. The running gel was prepared by adding the components of table XIII to a 15 ml tube and pipetting the mix between two glasses that were fixed in a standard. Subsequently, 1 ml of isopropanol was pipetted over the running layer to avoid bubbles in the gel and was removed after polymerization of the running gel.

Table XIII: Running and stacking mixes for one gel

Component	Volume (ml) Running mix	Volume (ml) Stacking mix
ddH$_2$O	2.39	1.52
Run Tris-SDS (Table I)	1.33	/
Stack Tris-SDS (Table I)	/	0.33
Acrylamide (30%) (Table I)	1.25	0.63
APS (10%) (Table I)	0.02	0.015
TEMED (Bio-Rad)	0.01	0.005
Final	**5**	**2.5**

The stacking mix (Table XIII) was then poured on the running gel and a comb was inserted. When polymerized, the comb was removed and the gel was put in a migration tank filled with migration buffer (Table I). 30 µg proteins of each sample was then loaded on the gel along with the Kaleidoscope protein marker (Bio-Rad) as standard and stacking of the proteins occurred at 75V for 30 minutes. Subsequently, the proteins were separated at 120V for 1 hour and were blotted onto a nitrocellulose membrane (GE Healthcare). For this blotting, the wet transfer method was used and a transfer sandwich was prepared in the following order: black frame (negative electrode) – foam – filter paper – gel – membrane – filter paper – transparent frame (positive electrode). Each component was initially equilibrated in transfer buffer (Table I) and then put into a transfer tank filled with this buffer. The transfer from the gel to the membrane occurred at 100 V for 2 hours in the cold room. To control the efficacy of the transfer, the membrane was stained with Ponceau red (Table I) and subsequently washed with distilled water. Then the membrane was blocked during 1 hour with 5% milk solution in Tris-Buffered-Saline (TBS, Table I)-Tween 1%. Upon blocking, the membrane was washed 6 x 10 minutes with TBS-Tween 1% and incubated overnight with the primary antibody at 4°C (table XIV). The next morning, the membrane was washed again 6 x 10 minutes with TBS-Tween 1% and incubated with the secondary antibody (table XIV) for 1 hour at RT. Finally, the membrane was washed again 6 x 10 minutes and incubated for 5 minutes with enhanced chemiluminiscent (ECL) substrate (Roche) before exposing it to the X-ray film and analysis for chemiluminiscence. The same membrane could be used for another primary antibody after thoroughly thoroughly with TBS-T 1% and addition of the antibody in a solution containing 5% milk and Azide (Sigma) (to block the horseradish peroxidase used for the first antibody).

As a control for equal protein-loading, a Western Blot was performed with a primary anti-glyceraldehyde 3-phosphate dehydrogenase (GAPDH) antibody (table XIV), which is a housekeeping gene.

Table XIV: Dilutions of antibodies used for Western Blot

Antibody	Dilution in 5% milk
Primary anti-COOH terminal XBP1 antibody (Biolegend)	1/500
Primary anti-BiP antibody (Cell Signaling Technology)	1/1000
Primary anti-GAPDH antibody (Sigma-Aldrich)	1/10.000
Secondary anti-rabbit (H+L) antibody (Jackson Immunoresearch)	1/20.000

XBP1, X-box binding protein 1; BiP, immunoglobulin-heavy-chain-binding protein; GAPDH, glyceraldehyde 3-phosphate dehydrogenase.

2.8   Processing of data and statistical analysis

The data obtained with flow cytometry, qPCR and ELISA were processed and statistically analysed with Graphpad Prism 5.1. The results were represented as the mean of cell amounts, OD-value or concentration ± SEM (errorbars in figure) in a bar chart. The groups were compared in pairs with a nonparametric two-tailed Mann-Withney U test, in which no Gaussian distribution was assumed. A P-value smaller than 0.05 is statistic significant and is represented with *, P-value < 0.01 with ** and P-value < 0.001 with ***.

3   Results

3.1   Genotype of the mice

To start, we sought to validate the CD11c Cre$^{-/+}$ XBP1$^{fl/fl}$ model. In this model, exon 2 of *Xbp1* is flanked by two LoxP sites resulting in the excision of this gene fragment and dysfunction of *Xbp1* when the Cre-recombinase is expressed (Figure 6). Since expression of the recombinase is restricted to CD11c positive cells, *Xpb1* should be dysfunctional in DCs.
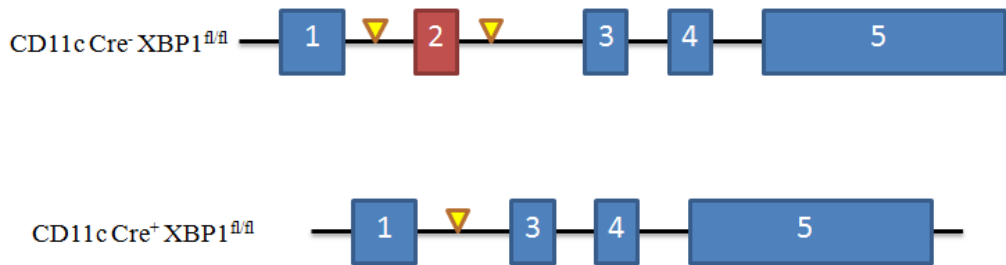
Figure 6: Schematic representation of the *Xbp1fl/fl* alleles from CD11c Cre⁻ XBP1fl/fl and CD11c Cre⁺ XBP1fl/fl mice. Exon 2 of *Xbp1* is flanked by two LoxP sites (presented as yellow triangles). When the Cre-recombinase is expressed, exon 2 is deleted and *Xbp1* is dysfunctional. Adapted from Hess *et al.* (69).

To validate this model, iDCs were generated after 8 days of culture with medium (TCM) containing 20 ng/ml of the growth factor GM-CSF. At day 3 and 6, fresh medium was added and RNA was extracted at day 8 (figure 7).
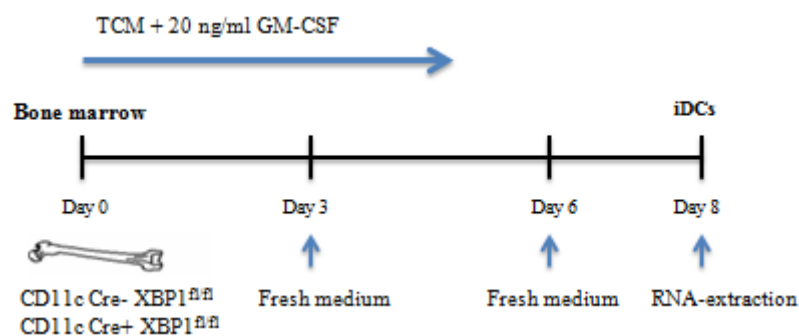
Figure 7: Experimental set-up bone marrow culture. Bone marrow cells isolated from the limbs of two types of mice (CD11c Cre⁻ XBP1fl/fl and CD11c Cre⁺ XBP1fl/fl) were plated in 100 mm culture dishes at a concentration of 2-3 x 10^6 cells in 10 ml tissue culture medium (TCM) containing 20 ng/ml granulocyte-macrophage colony-stimulating factor (GM-CSF). At day 3 and 6 of the culture, the medium was refreshed. After 8 days of culture, the generated inflammatory DCs (iDCs) were harvested, followed by the extraction of RNA.

Upon RNA-extraction and cDNA-production, qrt-PCR was done with primers that specifically recognize exon 2 of *Xbp1* (table V). We observed no exon 2 amplicon in CD11c Cre⁺ XBP1fl/fl DCs, as was expected (figure 8).
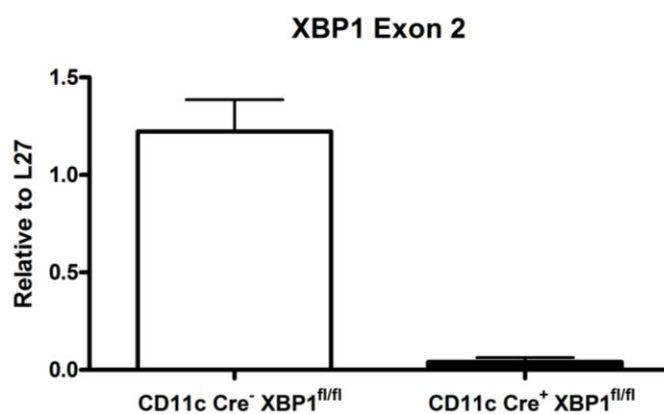
Figure 8: Genotype of the CD11c Cre⁺ XBP1^{fl/fl} mice. RNA was extracted from BMDCs of CD11c Cre⁻ XBP1^{fl/fl} and CD11c Cre⁺ XBP1^{fl/fl} mice and was compared for mRNA expression of exon 2 in *Xbp1* with qrt-PCR (n=1 for each mouse type). Data are represented as the mean of the duplicates $\pm$ SD and are relative to the mRNA expression of the housekeeping gene *L27*.

3.2   Induction of ER stress by the different stimuli

For most of the experiments, the PRR-agonists represented in table II, were used to stimulate and induce maturation of iDCs. Since activation of DCs is also associated with the induction of ER stress (42), we tested to what degree these PRR-stimuli are capable of triggering ER stress in iDCs. For this purpose, the iDCs were stimulated with PRR-ligands on day 8 of the culture and RNA was extracted after 6 hours. Induction of ER stress related genes was measured with qrt-PCR (Figure 9).

To correlate gene expression to protein expression level, Western Blot analysis was performed for some ER stress related genes (Figure 10). More specifically, BiP, EDEM (ER degradation-enhancing α mannosidase-like protein), SEC61 and XBP1 were analyzed. EDEM is a target of the IRE1-XBP1 pathway and up-regulation of this protein in the context of ER stress facilitates ER-associated protein degradation (ERAD) (70).

SEC61 on the other hand, mediates the translocation of proteins from the cytosol into the ER, but is also involved in the retro-translocation of ERAD substrates from the ER to the cytosol (71). Hence, up-regulation of these genes would indicate the induction of ER stress.
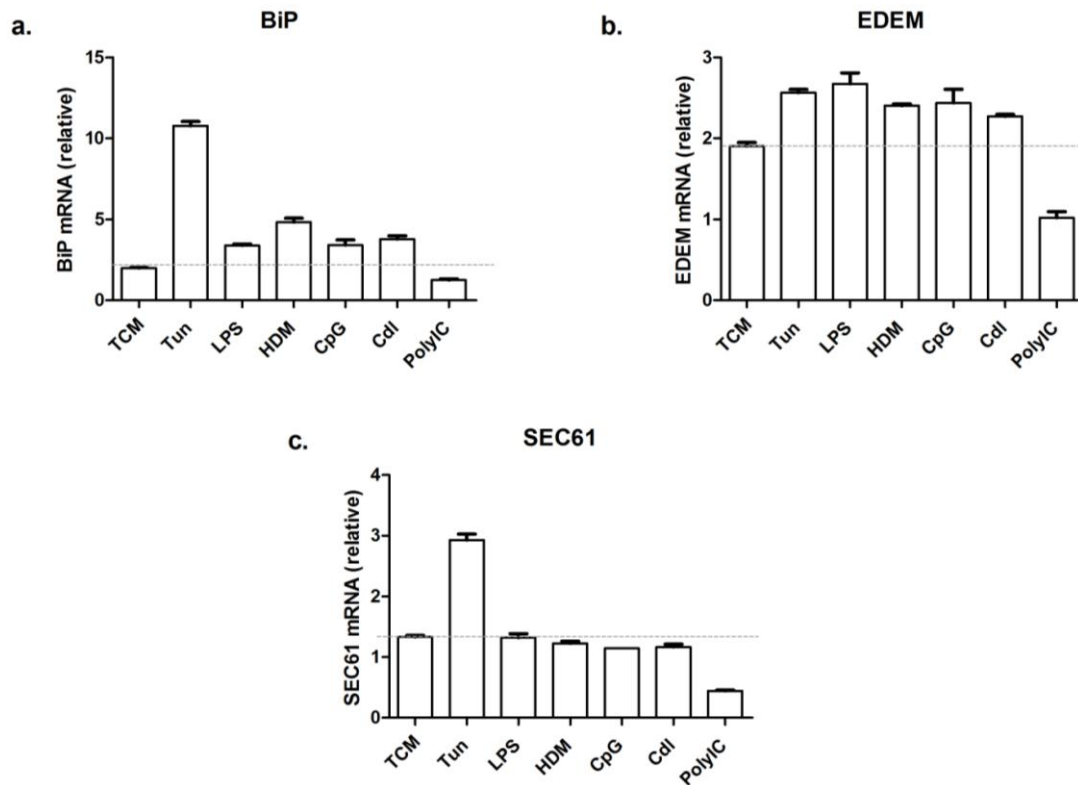
Figure 9: mRNA expression of ER stress related genes in CD11c Cre⁻ XBP1^fl/fl mice upon stimulation. RNA was extracted after 6 hours of stimulation of BMDCs of CD11c Cre⁻ XBP1^fl/fl mice and mRNA expression of ER stress related genes, *Bip* (a), *Edem* (b) and *Sec61* (c), was measured with qrt-PCR. Data are presented relative to *L27* (mean ± S.D. of duplicates). TCM, tissue culture medium; LPS, lipopolysaccharide; HDM, house dust mite; Cdl, curdlan; Tun, tunicamycin.

Tunicamycin is a commonly used ER stress inducer for *in vitro* experiments. It functions *via* inhibition of N-linked glycosylation, which is necessary to modify proteins and assures proper folding (49). This way, unfolded proteins will accumulate in the ER and ER stress will be induced. Tunicamycin was therefore used as a positive control for the presence of ER stress and mRNA expression in the different conditions was compared to the expression level in the untreated control (TCM, represented by the dotted line) to see induction of ER stress.

We observed an increase in *Bip* mRNA expression upon stimulation with LPS, HDM, CpG and curdlan (Figure 8a). HDM even induced a two-fold increase in *Bip* expression, which is highly interesting since HDM is a naturally occurring allergen and this effect has not yet been described in literature. In contrast, polyIC did not increase *Bip* mRNA expression, in fact, it appeared to reduce expression of this ER stress related gene.

For *Edem*, the expression levels were in line with those observed for *Bip* (Figure 8b) and were up-regulated when the iDCs were stimulated with LPS, HDM, CpG and curdlan. Again polyIC treatment decreased *Edem* mRNA expression.

Expression of *Sec61* on the other hand, was not modified by LPS, HDM, CpG and curdlan. Even more, polyIC had a negative effect (Figure 8c).

These qrt-PCR data are preliminary, but suggest a link between the PRR-signaling pathways that are activated upon ligation with LPS, HDM, CpG and curdlan (table II) and the UPR.

Subsequently, protein expression levels of XBP1 (figure 10a) and BiP (figure 10b) were determined by Western Blot. The BMDCs were stimulated for 8 hours (table II) and proteins were extracted. Initially, the protein concentration was determined with a Biorad Bradford Protein Assay and 30 μg of the protein lysates was loaded on the gel.
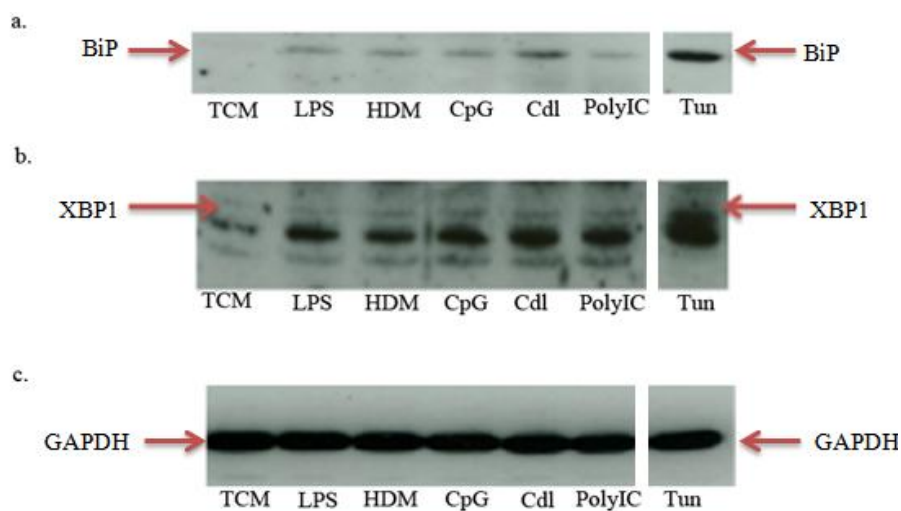

Figure 10: Protein expression of ER stress related genes in CD11c Cre⁻ XBP1^fl/fl mice upon stimulation. Proteins were extracted after 8 hours of stimulation of BMDCs of CD11c Cre⁻ XBP1^fl/fl mice and 30 μg of the protein lysates was loaded on an 8% gel. Protein expression of ER stress related genes, BiP (a) and XBP1 (b), was assessed with Western Blot. The results are representative of one experiment (a) or two independent experiments (b). Equal loading between samples was controlled with GAPDH (c). TCM, tissue culture medium; LPS, lipopolysaccharide; HDM, house dust mite; Cdl, curdlan; Tun, tunicamycin.

The Western Blot results for BiP (Figure 10a) confirm the qrt-PCR data (Figure 9a), showing up-regulation of BiP (78 kDa) upon PRR-ligation with LPS, HDM, CpG and curdlan, with the latter stimulant inducing the highest levels. Although we also observed a small band in the polyIC condition, this effect was only mild in comparison to the other conditions.

XBP1 expression was assessed using an antibody that binds to the COOH-terminal of the protein (55 kDa) (Figure 10b). We observed a small band in the untreated condition, indicating that XBP1 is basally present in iDCs, but XBP1 expression was enhanced after stimulation with LPS, HDM, CpG, curdlan and polyIC. Since the basal presence of XBP1 was

not reflected for BiP, it seems that the ER stress pathway was not fully activated at basal level. GAPDH is a housekeeping protein and was used as an internal control (Figure 10c) (72). As the blot showed no differences between samples, even loading, blotting and processing was confirmed.

Additionally, we performed a PCR with primers that bind to *Xbp1* sequences encompassing the region that is spliced out by *Ire1* (62), making it possible to detect both the spliced and unspliced form of *Xbp1* (Figure 11a).

When *Xbp1* splicing occurs, 26 base pairs are excised, converting a 171 bp fragment ($Xbp1_U$) in a 145 bp fragment ($Xbp1_S$) (73). In practice, after separation of the PCR products by electrophoresis through a 2.5% agarose gel, we should detect a second band with a lower molecular weight in case of ER stress (representing $Xbp1_S$),
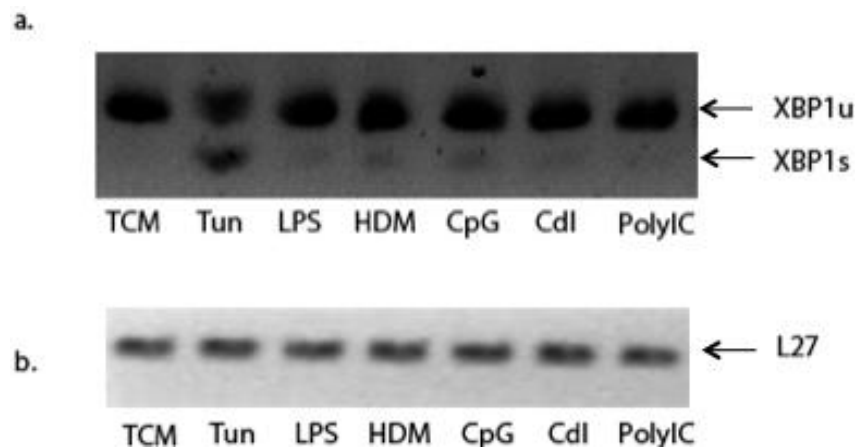

Figure 11: Splicing of XBP1 upon stimulation in CD11c Cre⁻ XBP1^fl/fl mice. RNA was extracted after 6 hours of stimulation of BMDCs of CD11c Cre⁻ XBP1^fl/fl mice and *Xbp1* splicing (a) was assessed with PCR. PCR analysis was done with a primer set flanking the spliced-out region in *XBP1s* mRNA. *L27* expression served as loading control (b). PCR products were resolved on a 2.5% agarose gel to separate unspliced (*Xbp1u*) and spliced (*Xbp1s*) *Xbp1* mRNAs. TCM, tissue culture medium; LPS, lipopolysaccharide; HDM, house dust mite; Cdl, curdlan; Tun, tunicamycin.

LPS, HDM, CpG and curdlan stimulated *Xbp1* splicing, although ligand-specific differences were observed. More specifically, mostly HDM and CpG induced enhanced splicing, whereas LPS and curdlan showed less expression of $Xbp1_S$. No basal *Xbp1* splicing was observed and *L27* expression was similar between samples, guaranteeing equal loading (Figure 10b).

Collectively, these data again point toward a cross-link between PRR-specific signaling pathways and the XBP1-pathway.

3.3 The role of XBP1 in the survival of iDCs

The goal of this experiment was to assess the potential role of XBP1 in the survival of iDCs. At day 8 of the bone marrow culture, the final yield was first determined with trypan blue (Figure 12).
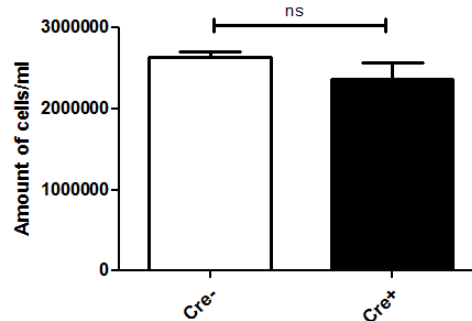

Figure 12: Final yield of the bone marrow culture at day 8. Bone marrow cells isolated from the limbs of two types of mice (CD11c Cre⁻ XBP1^{fl/fl} and CD11c Cre⁺ XBP1^{fl/fl}) were plated in 100 mm culture dishes at a concentration of 2-3 x 10⁶ cells in 10 ml TCM containing 20 ng/ml GM-CSF. After 8 days of culture, iDCs were harvested and the final yield of the culture was assessed with trypan blue. Data are represented as mean ± SEM of n=3 CD11c Cre⁻ XBP1^{fl/fl} and n=3 Cre+, CD11c Cre⁺ XBP1^{fl/fl} mice. Ns, non significant (Man-Whitney test); Cre-, CD11c Cre⁻ XBP1^{fl/fl}; Cre+, CD11c Cre⁺ XBP1^{fl/fl}.

We observed no significant difference in the final yield of the bone marrow culture at day 8 between the two groups (Figure 12). Both types of DCs also showed normal development, as microscopic analysis of the cultures did not show any differences, exluding a key role for XBP1 in iDC development.

Additionally, the cells were analysed with flow cytometry. For this purpose, the cells were stimulated with different stimuli (table II), or with TCM as a negative control at day 8 of the culture. After 24 hours of stimulation, the frequency of alive cells vs. non-debris was determined with flow cytometry (Figure 13).
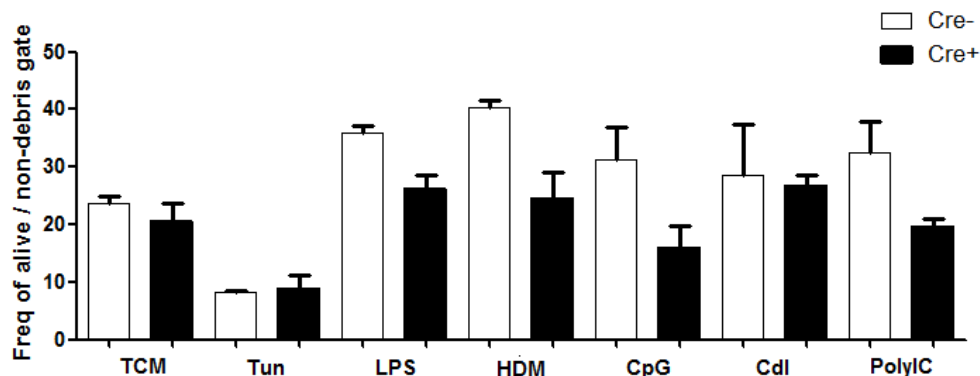

Figure 13: Frequency of alive cells vs. non-debris. Flow cytometry was done after 24 hours of stimulation of BMDCs of CD11c Cre⁻ XBP1^{fl/fl} and CD11c Cre⁺ XBP1^{fl/fl} mice. Live/dead cells were determined with Amcyan and the frequency of alive cells in the non-debris gate was determined with Flow Jo. Data are

presented as mean ± SEM for n = 2 CD11c Cre$^-$ XBP1$^{fl/fl}$ and n = 2 CD11c Cre$^+$ XBP1$^{fl/fl}$ mice. TCM, tissue culture medium; LPS, lipopolysaccharide; HDM, house dust mite; Cdl, curdlan; Tun, tunicamycin; Cre-, CD11c Cre$^-$ XBP1$^{fl/fl}$; Cre+, CD11c Cre$^+$ XBP1$^{fl/fl}$.

In the untreated condition (TCM), we observed no difference in survival between the WT and XBP1-deficient DCs, which supports the results from the trypan blue analysis and indicates normal basal survival and development in both groups. Also upon tunicamycin treatment, no clear difference was observed. Remarkably, the frequencies of alive cells were much lower in this condition compared to all the other conditions, indicating the harmful effect of ER stress on DCs. Upon stimulation with LPS, HDM, CpG and polyIC, the XBP1-deficient DCs appeared to survive less than their WT counterparts, albeit the observed effect is mild. Curdlan treatment on the other hand, did not induce a difference in survival between both groups. Together, these results do not provide evidence for an essential role of XBP1 in iDC survival.

3.4 The role of XBP1 in the maturation and normal function of iDCs

Maturation of DCs is a process of differentiation in which the DC transforms from a celltype that is specialized in the up-take of antigens to a celltype that is specialized in the stimulation of T-cells. This process is among others associated with increased expression of co-stimulatory molecules CD40 and CD86 (2). Therefore, expression of these molecules was determined with flow cytometry to assess the potential role of XBP1 on the maturation of inflammatory DCs (Figure 14, 15).
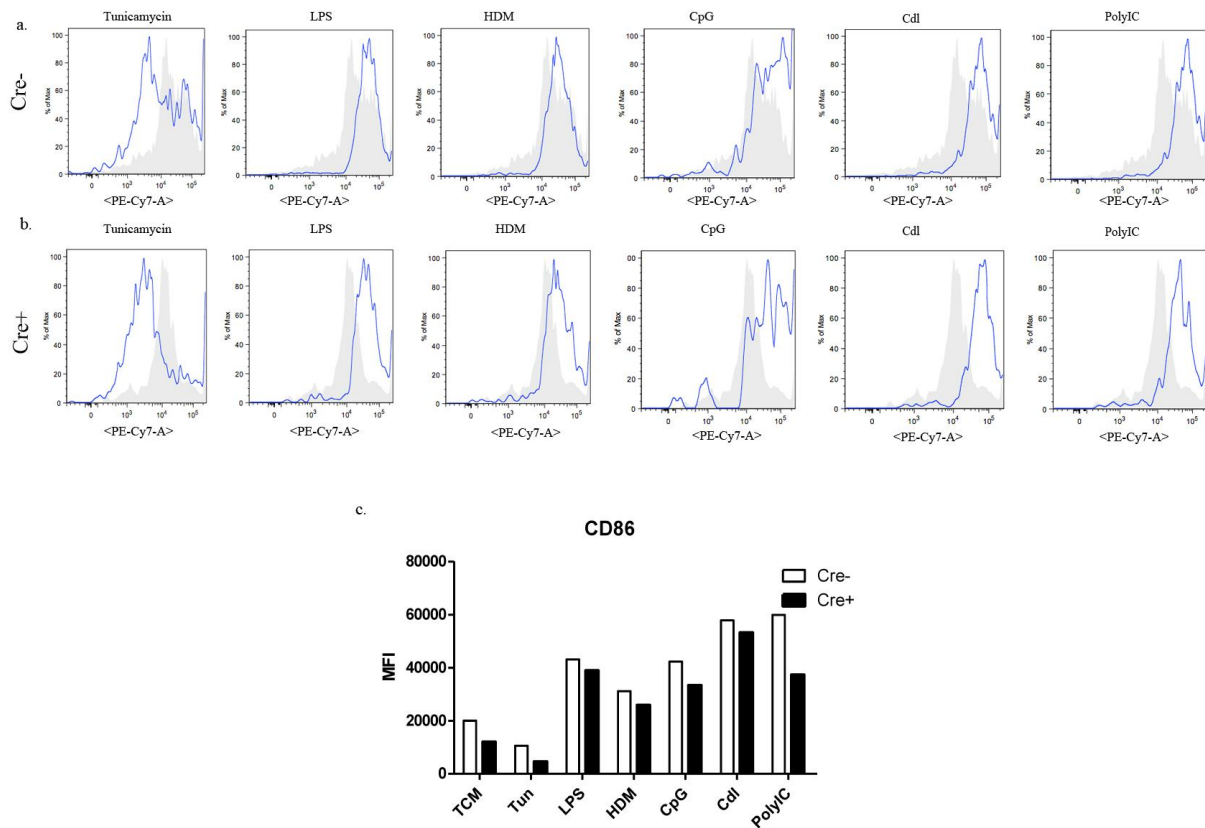
Figure 14: Maturation of CD11c Cre⁻ XBP1ᶠˡ/ᶠˡ and CD11c Cre⁺ XBP1ᶠˡ/ᶠˡ mice. Flow cytometry was done after 24 hours of stimulation of the BMDCs of CD11c Cre⁻ XBP1ᶠˡ/ᶠˡ (a) and CD11c Cre⁺ XBP1ᶠˡ/ᶠˡ (b) mice. Cells were stained with anti-CD11c, anti-CD86 and anti-CD40. Amcyan was used as live/dead marker. The results represent CD86 expression of alive, CD11c⁺ cells. For every condition, expression of CD86 is depicted by the blue graphs and compared to its expression in the untreated condition, TCM (shaded). The (geometric) mean fluorescence intensity (MFI) is presented in (c). The data are representative of 2 independent experiments. TCM, tissue culture medium; LPS, lipopolysaccharide; HDM, house dust mite; Cdl, curdlan; Tun, tunicamycin; Cre-, CD11c Cre⁻ XBP1ᶠˡ/ᶠˡ; Cre+, CD11c Cre⁺ XBP1ᶠˡ/ᶠˡ.
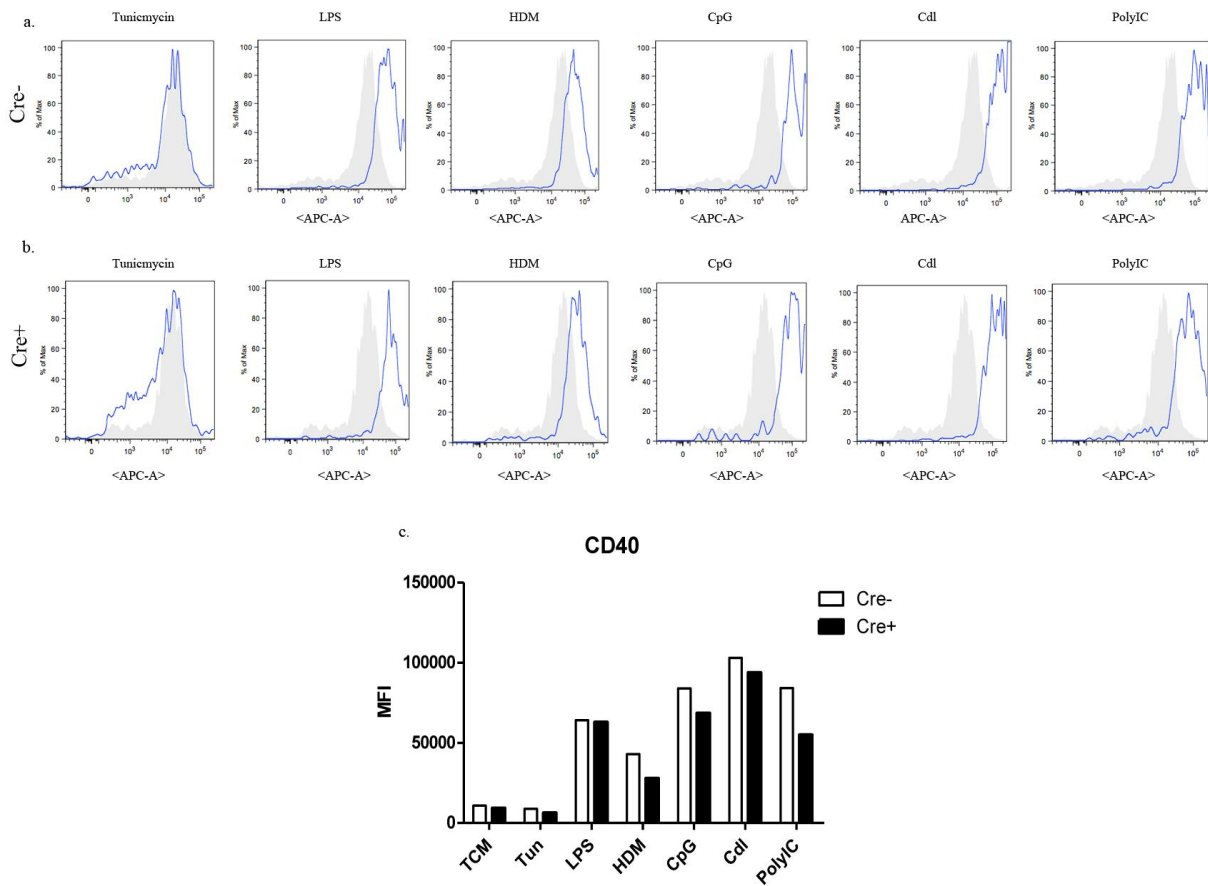
Figure 15: Maturation of CD11c Cre⁻ XBP1^fl/fl and CD11c Cre⁺ XBP1^fl/fl mice. Flow cytometry was done after 24 hours of stimulation of BMDCs of CD11c Cre⁻ XBP1^fl/fl (a) and CD11c Cre⁺ XBP1^fl/fl (b) mice. Cells were stained with anti-CD11c, anti-CD86 and anti-CD40. Amcyan was used as live/dead marker. The results represent CD40 expression of alive, CD11c⁺ cells. For every condition, expression of CD40 is depicted by the blue graphs and compared to its expression in the untreated condition (shaded). The (geometric) mean fluorescence intensity (MFI) is presented in (c). The data are representative of 2 independent experiments. TCM, tissue culture medium; LPS, lipopolysaccharide; HDM, house dust mite; Cdl, curdlan; Tun, tunicamycin; Cre-, CD11c Cre⁻ XBP1^fl/fl; Cre+, CD11c Cre⁺ XBP1^fl/fl.

Upon tunicamycin stimulation, CD86 expression was reduced in both groups (Figure 14a, b, c) compared to the untreated condition, which supports the results from the survival analysis (Figure 13) and suggests a toxic effect of tunicamycin on DCs or down-regulation of maturation markers in response to acute ER stress. LPS, HDM, CpG, curdlan and polyIC stimulated higher expression of CD86 in both groups, confirming the capacity of these stimuli to promote DC survival. Since CD86 expression was increased to a similar extent in both groups, XBP1-deficiency probably does not have an impact on iDC survival upon PRR-stimulation.

We observed similar results for CD40 expression, again showing no differences in iDC survival upon stimulation with LPS, HDM, CpG, Cdl and polyIC between the two groups and therefore excluding an important role for XBP1 in this process (Figure 15a, b, c).

Although there is a minor decrease in mean fluorescence intensity (MFI) of CD86 and CD40 in the XBP1-deficient DCs (Figure 14c, 15c), it is not clear at this point whether this is significant.

Maturation and normal function of DCs is also associated with secretion of cytokines. Dependent on the secreted cytokine, the T-cell response is polarized to Th1, Th2, Th17 or Treg cells, thereby determining the ensuing immune response. Analysis of mRNA-expression (Figure 16a, 17a, 18a) and production (Figure 16b, 17b, 18b) of IL-6, IL-10, IL-12 and TNF is therefore a good manner to assess maturation of the iDCs.

At day 8 of the culture, iDCs were stimulated (table II), or untreated as a negative control and RNA was extracted after 3, 6 and 9 hours of stimulation. This way, the mRNA expression profile could be followed in time.

Subsequently, the presence of certain cytokines in the supernatant of the bone marrow culture was assessed with ELISA. More specifically, the production of IL-6 (Figure 16b), IL-12 (Figure 17b), TNF (Figure 18b) and IL-10 (Figure 19) was measured. For this experiment, the iDCs were stimulated (table II), or unstimulated (TCM) at day 8 of the culture and ELISA was done after 24 hours of stimulation.
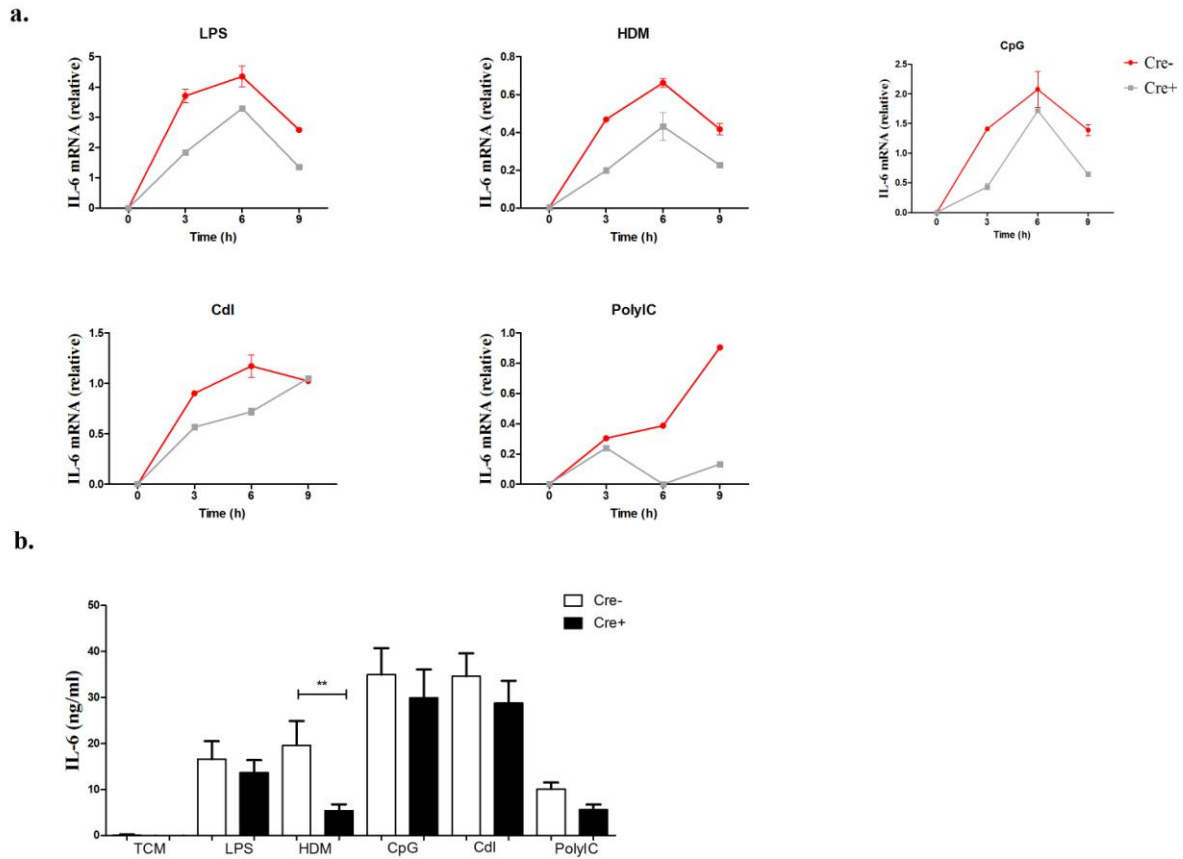
Figure 16: IL-6 secretion. (a) Qrt-PCR analysis of *Il-6* mRNA from BMDCs obtained from CD11c Cre⁻ XBP1^fl/fl (Cre-) and CD11c Cre⁺ XBP1^fl/fl (Cre+) mice and stimulated with nothing (TCM), LPS, HMD, CpG, Cdl or PolyIC, assessed over a time course of 0-9 hours. Results are presented relative to *L27* (mean ± S.D. of duplicates). Data are from one representative of three independent experiments. (b) ELISA analysis of IL-6 production (ng/ml) in supernatants of the BMDCs in (a) assessed at 24 hours. Data are represented as mean ± SEM of n=3 CD11c Cre⁻ XBP1^fl/fl and n=3 Cre+, CD11c Cre⁺ XBP1^fl/fl mice. ** P < 0.01 (Man-Whitney test). TCM, tissue culture medium; LPS, lipopolysaccharide; HDM, house dust mite; Cdl, curdlan; Tun, tunicamycin.

XBP1-deficient iDCs stimulated with PRR-agonists (table II) showed an overall impairment in *Il-6* mRNA production (Figure 16a) and IL-6 secretion (Figure 16b), as measured by qrt-PCR and ELISA respectively. Though, the severity of impairment was ligand-specific and the most striking result was observed with HDM. XBP1-deficiency led to a relative decrease in *Il-6* mRNA expression upon HDM stimulation that was similar to the decrease observed after LPS stimulation. Of this latter, the dependence on XBP1 to ensure sustained production of IL-6 was already shown in macrophages (62) and was here extrapolated to iDCs.

The ELISA results also showed a significant decrease in IL-6 secretion upon HDM stimulation in iDCs lacking XBP1 (Figure 16b), confirming the qrt-PCR data at protein level.

PolyIC-triggering was affected as well by the absence of XBP1 for the induction of *Il-6* expression (Figure 16a). However since polyIC was not included in all experiments, further research should be attended.

The ligands CpG and curdlan on the other hand, were less dependent on XBP1 for *Il*-6 expression, since the differences between WT and XBP1-deficient iDCs were milder and time point-specific (Figure 16a). This was also reflected by the ELISA results, expanding the mRNA expression data to protein levels (Figure 16b).

In conclusion, HDM and LPS showed an impaired capacity to induce *Il-6* expression in XBP1-deficient iDCs and are therefore likely to require XBP1 for optimal expression of this cytokine.
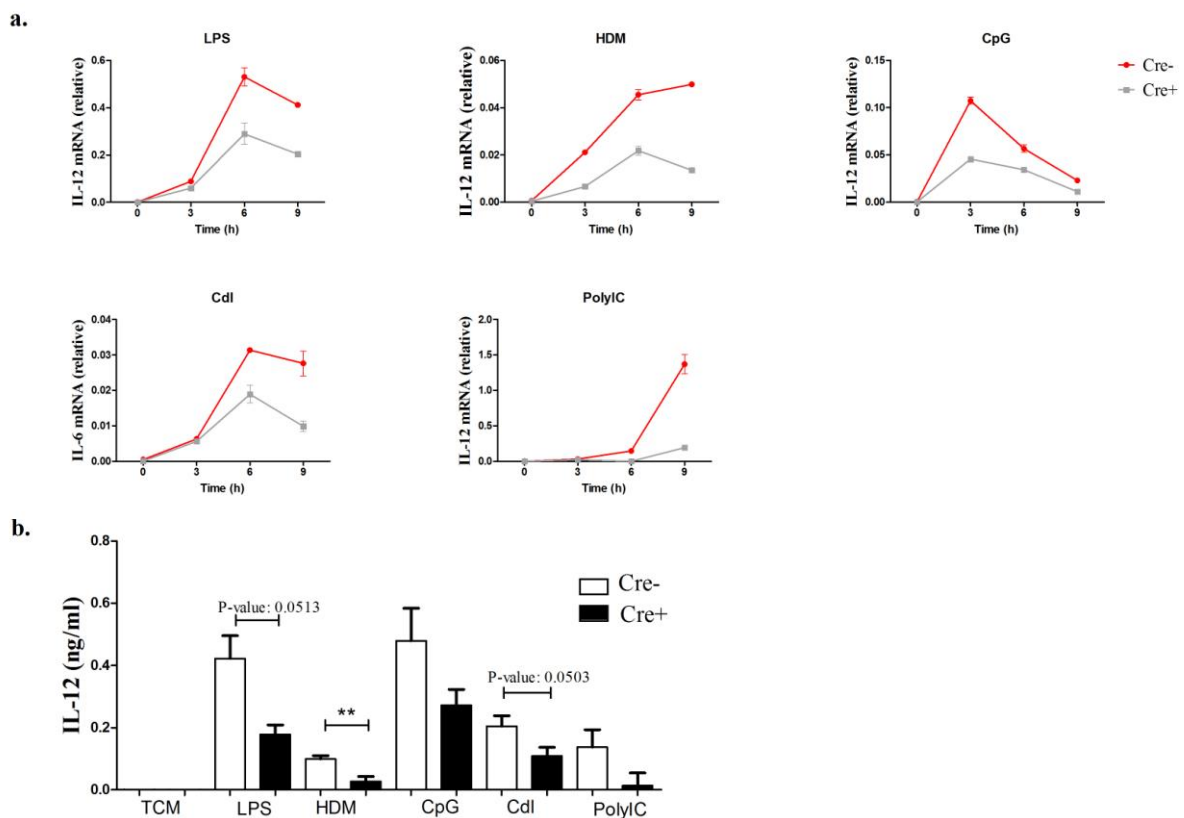

Figure 17: IL-12 secretion. (a) Quantitative real-time PCR analysis of *Il-12* mRNA from BMDCs obtained from CD11c Cre⁻ XBP1^fl/fl (Cre-) and CD11c Cre⁺ XBP1^fl/fl (Cre+) mice and stimulated with nothing (TCM), LPS, HMD, CpG, Cdl or PolyIC, assessed over a time course of 0-9 hours. Results are presented relative to *L27* (mean ± S.D. of duplicates). Data are from one representative of three independent experiments. (b) ELISA analysis of IL-12 production (ng/ml) in supernatants of the BMDCs in (a) assessed at 24 hours. Data are represented as mean ± SEM of n=3 CD11c Cre⁻ XBP1^fl/fl and n=3 Cre+, CD11c Cre⁺ XBP1^fl/fl mice. ** $P < 0.01$ (Man-Whitney test). TCM, tissue culture medium; LPS, lipopolysaccharide; HDM, house dust mite; Cdl, curdlan; Tun, tunicamycin.

Il-12 mRNA expression analysis also demonstrated a ligand-dependent decrease in XBP1-deficient iDCs (Figure 17a). More specifically, LPS, HDM and curdlan showed reduced capacity to induce *Il-12* expression in these cells, as measured by qrt-PCR. CpG and polyIC showed differences as well, but the effects were less pronounced and polyIC-induced *Il-12* expression was only observed in the WT iDCs upon 9 hours of stimulation.

The ELISA results confirmed these data at protein level (Figure 17b) suggesting that LPS, HDM and curdlan require XBP1 to produce optimal levels of IL-12.
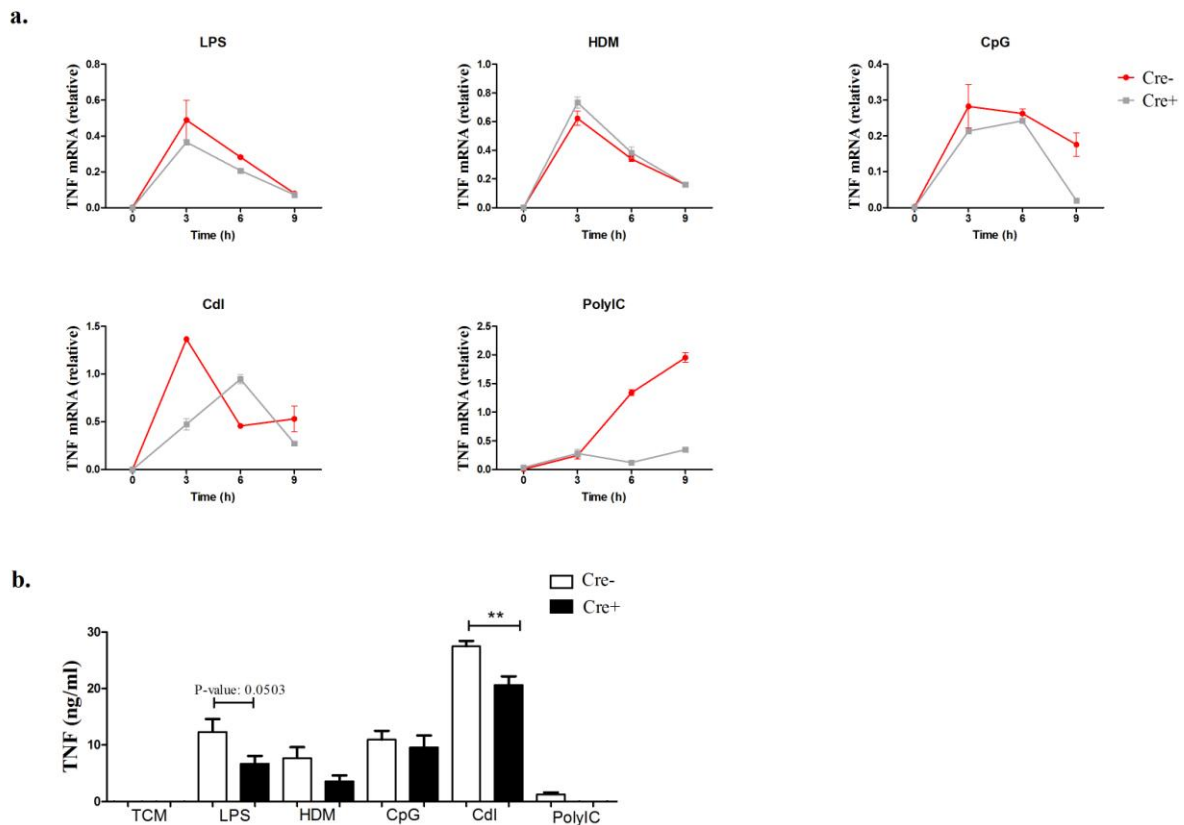

Figure 18: TNF secretion. (a) Qrt-PCR analysis of *Tnf* mRNA from BMDCs obtained from CD11c Cre⁻ XBP1^fl/fl (Cre-) and CD11c Cre⁺ XBP1^fl/fl (Cre+) mice and stimulated with nothing (TCM), LPS, HMD, CpG, Cdl or PolyIC, assessed over a time course of 0-9 hours. Results are presented relative to *L27* (mean ± S.D. of duplicates). Data are from one representative of three independent experiments. (b) ELISA analysis of TNF production (ng/ml) in supernatants of the BMDCs in (a) assessed at 24 hours. Data are represented as mean ± SEM of n=3 CD11c Cre⁻ XBP1^fl/fl and n=3 Cre+, CD11c Cre⁺ XBP1^fl/fl mice. ** P < 0.01 (Man-Whitney test). TCM, tissue culture medium; LPS, lipopolysaccharide; HDM, house dust mite; Cdl, curdlan; Tun, tunicamycin.

We observed no clear differences in *Tnf* mRNA expression between both groups of DCs upon stimulation with LPS, HDM and CpG (Figure 18a), which suggests that XBP1 is involved in the expression of a specific subset of cytokines. Though for curdlan, differences in kinetics of *Tnf* expression were observed, as we detected a later and lower peak of expression in XBP1-

deficient iDCs compared to WT iDCs. This was supported by the ELISA results, showing a significant decrease in TNF-production upon stimulation with curdlan in XBP1-deficient iDCs (Figure 18b), indicating XBP1-dependence of this PRR-ligand to produce TNF.

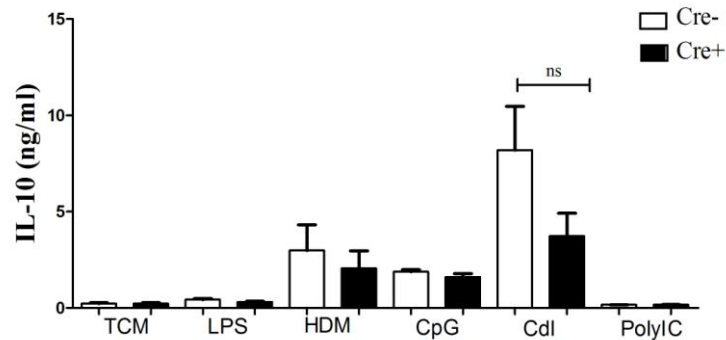Finally, IL-10 production upon PRR-stimulation was assessed with ELISA (Figure 19).

Figure 19: IL-10 secretion. ELISA analysis of IL-10 production (ng/ml) in supernatants of BMDCs obtained from CD11c Cre⁻ XBP1^{fl/fl} (Cre-) and CD11c Cre⁺ XBP1^{fl/fl} (Cre+) mice and stimulated for 24 hours with nothing (TCM), LPS, HMD, CpG, Cdl or PolyIC. Data are represented as mean ± SEM of n=3 CD11c Cre⁻ XBP1^{fl/fl} and n=3 Cre+, CD11c Cre⁺ XBP1^{fl/fl} mice. Ns, non significant (Man-Whitney test). TCM, tissue culture medium; LPS, lipopolysaccharide; HDM, house dust mite; Cdl, curdlan; Tun, tunicamycin.

We observed no significant differences in IL-10 production between both groups in all conditions. This suggests that LPS-, HDM-, CpG-, Cdl- and polyIC-triggered IL-10 production is not likely to depend on XBP1.

All together, these cytokine analyses suggest a PRR- and mediator-specific dependence on the IRE1-XBP1 branch of the UPR.

3.5 Effect of XBP1-deficiency on ER stress management in inflammatory DCs

To assess the effect of XBP1-deficiency on the management of ER stress in iDCs, BMDCs deficient or not for XBP1 were subjected on day 8 of culture to tunicamycin. RNA was extracted after 6 hours of stimulation and qrt-PCR was performed to measure the gene induction of ER stress related genes (Figure 20). More specifically, mRNA expression profiles of *Edem, Sec61* and *Bip* should reflect their response to ER stress.
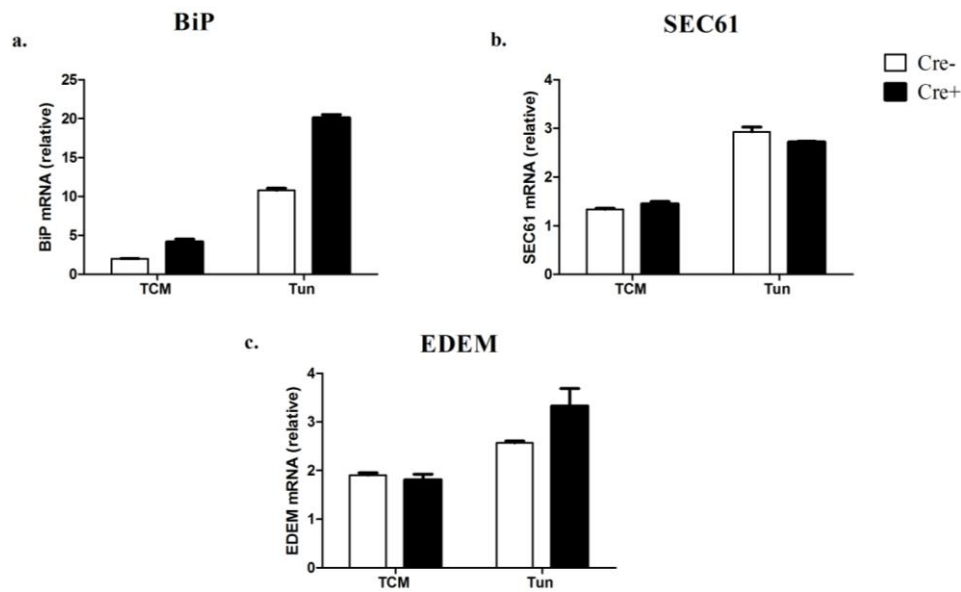
Figure 20: mRNA expression of ER stress related genes. Qrt-PCR analysis of ER stress related genes, *Sec61* (a), *Edem* (b) and *Bip* (c) from BMDCs obtained from CD11c Cre⁻ XBP1^{fl/fl} (Cre-) and CD11c Cre⁺ XBP1^{fl/fl} (Cre+) mice and stimulated with tunicamycin for 6 hours. Data are from one representative of three independent experiments and are presented relative to *L27* (mean ± S.D. of duplicates). TCM, tissue culture medium; Tun, tunicamycin.

Subsequently, a Western Blot analysis of BiP was done to address the effect of XBP1-deficiency on ER stress management at protein level (Figure 21). BMDCs of the two types (CD11c Cre^{-/+} XBP1^{fl/fl}) were stimulated for 8 hours with tunicamycin or left untreated (TCM) and proteins were extracted. Protein concentration was first determined with a Biorad Bradford Protein Assay and 30 µg of protein lysates was loaded on the gel.
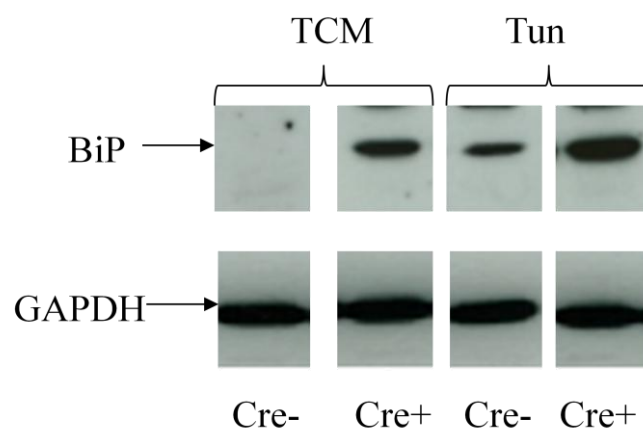
Figure 21: BiP production. Proteins were extracted after 8 hours of stimulation of BMDCs of CD11c Cre⁻ XBP1^{fl/fl} and CD11c Cre⁺ XBP1^{fl/fl} mice with tunicamycin or TCM (negative control) and 30 µg of the protein lysates was loaded on the gel. Protein expression of BiP was assessed with Western Blot. Data are representative of 3 independent experiments. Cre⁻, CD11c Cre⁻ XBP1^{fl/fl}; Cre⁺, CD11c Cre⁺ XBP1^{fl/fl}; Tun, tunicamycin; TCM,

tissue culture medium; BiP, immunoglobulin-heavy-chain-binding protein; GAPDH, glyceraldehyde 3-phosphate dehydrogenase.

The qrt-PCR data showed up-regulation of *Bip* in XBP1-deficient iDCs with (Tun) and without (TCM) stimulation compared to WT iDCs (Figure 20a). This was reflected by the Western Blot results (Figure 21), showing no basal presence of BiP in WT iDCs, in contrary to the XBP1-deficient iDCs. Tunicamycin treatment induced up-regulation of BiP in both groups, but reached higher levels in the XBP1-deficient iDCs.

This difference in up-regulation between both groups was only mildly observed for *Edem* upon tunicamycin treatment, but not in the untreated condition (Figure 20c) and *Sec61* expression levels did not show any differences (Figure 20b). These results indicate that the imbalance in ER stress due to XBP1-deficiency, encompass some but not all members of the UPR.

4   Discussion

ER stress and the UPR have become an extensively studied subject in today's research since there is increasing evidence for this pathway to be involved in diverse diseases, such as type 1 diabetes, neurodegenerative diseases, cardiovascular diseases and autoimmune diseases (51, 66). In this thesis, the role of the UPR and more specifically of the IRE1-XBP1 branch, in iDCs was studied with mice that had a CD11c-specific deletion of *Xbp1*.

In a first section, the potential cross-link between PRR-signaling and the UPR in iDCs was tested by assessing the levels of expression of ER stress related genes or proteins, such as BiP, EDEM, XBP1 and SEC1 by qrt-PCR, Western Blot and regular PCR.

A second part focused on the identification of a potential role for XBP1 in iDC survival, maturation and function upon stimulation with various PRR-ligands.

Finally, we examined the effect of XBP1-deficiency on ER stress management in iDCs to elucidate the importance of XBP1 in the maintenance of ER homeostasis.

4.1   Specific PRR-agonists trigger UPR activation in iDCs.

Recent studies have reported transcriptional up-regulation of XBP1 in murine macrophages upon LPS stimulation (62). Our results confirm these findings in iDCs and extend it to implicate more PRR-signaling pathways and ER stress related genes. More specifically, we observed up-regulation of XBP1 (Figure 10b) and its ER stress target genes *Edem* (Figure 9b) and *Bip* (Figure 9a, on protein level as well, Figure 10a) when subjected to LPS, but also to

HDM, CpG oligodeoxynucleotides and curdlan. PolyIC did not reproduce these observations, confirming previous results from Hu *et al.* who showed no induction of ER-resident chaperones, grp78 and grp170 upon DC stimulation with polyIC. *Sec61* expression was not altered after triggering with any of the PRR-ligands (Figure 9c), suggesting that this ER stress gene is regulated *via* an alternative signaling pathway.

The Western Blot results showed a very mild, basal expression of XBP1 (Figure 10b), though this was not reflected by *Xbp1* splicing (Figure 11a), or other ER stress related genes, indicating that it was most likely an immature form of XBP1 that was detected basally. Hence, the results suggest that constitutive activation of XBP1 was absent in iDCs, which stands in marked contrast to pDCs (61). Nevertheless, when iDCs were stimulated with LPS, HDM, CpG, curdlan and polyIC, enhanced expression of XBP1 was observed and this was reproduced by BiP (Figure 10a), with curdlan having the most pronounced effect for this latter ER stress protein.

Finally, *Xbp1* splicing data reflected these preceding results and indicated enhanced splicing upon PRR-triggering with LPS, curdlan and even more with HDM and CpG.

These observations revealed a highly interesting, unsuspected capacity of HDM to trigger ER stress. Since it is a naturally occurring allergen that represents a significant determinant in asthma development (74), these results could be of importance for future research in asthma development and therapy. Since HDM can trigger both TLR-4 and the C-type lectin receptor Dectin-2 on the surface of DCs (75), further research on the contribution of each of these PRR-pathways to the stimulation of ER stress is suggested.

Together, these results suggest an interconnection between PRR-signaling and the ER stress response, though not all PRR-pathways have similar effects upon activation. Indeed, the MDA-5 and TLR-3 pathways that are activated upon polyIC-stimulation, showed to induce virtually no ER stress, which was in contrary to the TLR-4, Dectin-2, Dectin-1, and TLR-9 pathways (respectively activated by LPS, HDM, curdlan and CpG).

4.2   The role of XBP1 in survival of iDCs

The study of the potential role of XBP1 in iDCs started with the identification of its contribution to iDC survival. Our results showed no significant differences in survival rate between WT and XBP1-deficient iDCs when they were untreated (Figure 12, 13 TCM condition), excluding a key role for XBP1 in the basal survival of iDCs. This is not reflected by pDCs and cDCs as demonstrated by Iwakoshi *et al.* (61), who showed a marked reduction in cDCs and especially pDCs in XBP1$^{-/-}$/RAG-2$^{-/-}$ mice without stimulation. These seemingly

contradictory results could be explained by the time difference in XBP1 deletion between both mouse models. More specifically, in the mice used by Iwakoshi *et al.*, *Xbp1* was deleted entirely from the beginning of development, while in our experiments, *Xbp1* was not deleted before CD11c was expressed, which is later in development.

Since PRR-triggering promotes DC survival, we additionally assessed the effect of XBP1-deficiency on iDC survival upon exposure to LPS, HDM, CpG, curdlan and polyIC (Figure 13). As suspected, we observed an overall increase in survival rate of WT iDCs in these conditions, though the effect of curdlan was less pronounced. XBP1-deficient iDCs on the other hand, showed more resistance to the provided survival signals, however this effect was only mild and it is not clear at this point whether this is significant.

Tunicamycin was additionally included to illustrate the effect of ER stress on iDC survival, which was detrimental as both groups iDCs survived markedly less when compared to untreated iDCs. Interestingly, the harmful effects of tunicamycin on iDC survival were to a similar extent in both groups, suggesting that XBP1 does not play an essential role in the survival of iDCs upon ER stress. These results are however preliminary and should be further investigated as they are in contrast to previous results (61).

Overall, our results did not provide clear evidence for XBP1 to be essential in the survival of iDCs.

4.3   The role of XBP1 in the maturation and normal function of iDCs.

Maturation of DCs is essential for the induction of adaptive immunity and is characterized by an increase of T cell co-stimulatory molecules and the secretion of cytokines (cf. introduction). Dysregulation of these features has been shown to be involved in many diseases such as autoimmune and inflammatory diseases (76, 77), making it highly interesting to investigate the role of XBP1 in the maturation of iDCs. The first feature, namely up-regulation of co-stimulatory molecules CD40 and CD86, was induced by subjecting iDCs to distinct PRR-ligands (LPS, HDM, CpG, curdlan and polyIC). Overall, maturation was similarly induced in both groups (Figure 14, 15), indicating that XBP1 is not a critical component in iDC maturation. This was in contrast to previous studies on pDCs, which were found to be in a hyper-activated state in the absence of XBP1, as they constitutively expressed higher levels of CD86 and MHC class II molecules compared to the control mice (61). The iDCs were also treated with tunicamycin to determine the effect of ER stress on iDC maturation. Since expression of maturation markers was decreased in both groups, this provides additional evidence of the damaging effects of ER stress on DCs.

In contrast to the similar expression of maturation markers in both groups, XBP1-deficiënt iDCs did show impaired capacity to secrete specific cytokines upon stimulation with certain PRR-ligands. More specifically, IL-6 mRNA expression and protein secretion was diminished upon iDC stimulation, especially with HDM and LPS, in the absence of XBP1 (Figure 16). This was also observed for IL-12, although curdlan additionally showed decreased capacity to induce secretion of this cytokine in XBP1-deficient iDCs (Figure 17). Conversely, TNF-production was only diminished after treatment with curdlan in the XBP1-deficient group (Figure 18) and IL-10 secretion was not altered in any condition between both groups (Figure 19). Since each stimulus triggers distinct PRR-signaling pathways, these observations could be extended in view of the identification of a potential inter-connection between XBP1 and different PRR pathways. As LPS and HDM both trigger TLR-4, this pathway is likely to need XBP1 for optimal induction of cytokine secretion. Though, HDM additionally activates the C-type lectin receptor Dectin-2 (78), raising the question which pathway communicates with XBP1 upon HDM-ligation, if not both. Since HDM is of significant importance in the development of asthma and other allergic diseases, further research to address this question is suggested. Finally, Dectin-1, triggered by curdlan, also showed to require XBP1 for optimal secretion of IL-12.

These findings reflect the inter-connection between PRR-signaling and the UPR that was suggested in the first section of the discussion. The detection that specific PRR-ligands induced expression of ER stress markers together with the observed decrease in secretion of cytokines upon stimulation with these PRR-ligands in XBP1-deficient iDCs, indicate the presence of downstream effectors of PRRs that mediate ER stress and that need XBP1 for optimal iDC function.

4.4   Effect of XBP1-deficiency on ER stress management in iDCs.

Since XBP1 regulates transcription of a set of genes that are involved in the constitutive preservation of ER homeostasis in all cell types, the effect of XBP1-deletion on ER stress management in iDCs was addressed. Our results revealed that unstimulated XBP1-deficient iDCs spontaneously exhibited relative high levels of BiP, compared to WT iDCs (Figure 20, 21). Nevertheless, this was not reproduced by *Edem* and *Sec61* (Figure 20), indicating that the basal levels of ER stress caused by XBP1-deletion were limited to certain stress markers. These observations were also reported for intestinal epithelial cells, showing elevated basal levels of *Bip* and *Chop* when XBP1 was deleted (79). ER stress induction by tunicamycin up-regulated *Bip, Edem* and *Sec61* expression in both groups, although especially *Bip* and to a

lesser extent *Edem,* showed higher up-regulation in the XBP1-deficient iDCs. We conclude that ER stress is imbalanced in the absence of XBP1 in iDCs, although not all ER stress targets are implicated.

4.5   General conclusion

Overall, we concluded that specific PRR-pathways are inter-connected with the UPR in iDCs, since inflammation (here simulated by exposure to LPS, HDM, CpG or curdlan) caused up-regulation of ER stress markers. This connection was additionally reflected by the requirement of XBP1 for optimal cytokine secretion by iDCs upon inflammation. However, additional research in the identification of XBP1-mediating downstream effectors of PRRs in iDCs is suggested. Our results provide a first evidence for HDM to communicate with XBP1 for the induction of optimal iDC-secretion of IL-6 and IL-12. This could represent the onset of further research in asthma development and therapy. Furthermore, XBP1 appeared to be required for the constitutive maintenance of ER homeostasis.

5   <u>References</u>

1.   Oberdan, L., A. Cunningham, and P. L. Stern. 2011. Vaccine immunology. *Understanding modern vaccines, perspectives in vaccinology* 1:25-59.
2.   Murphy, K., P. Travers, and M. Walport. 2008. Janeway's immuno biology. Seventh edition.
3.   Niyonsaba, F., and H. Ogawa. 2005. Protective roles of the skin against infection: implication of naturally occurring human antimicrobial agents beta-defensins, cathelicidin LL-37 and lysozyme. *J Dermatol Sci* 40:157-168.
4.   Akira, S. 2009. Innate immunity to pathogens: diversity in receptors for microbial recognition. *Immunol Rev* 227:5-8.
5.   Bianchi, M. E. 2007. DAMPs, PAMPs and alarmins: all we need to know about danger. *J Leukoc Biol* 81:1-5.
6.   Medzhitov, R., and C. A. Janeway, Jr. 1998. Innate immune recognition and control of adaptive immune responses. *Semin Immunol* 10:351-353.
7.   Medzhitov, R., and C. Janeway, Jr. 2000. Innate immunity. *N Engl J Med* 343:338-344.
8.   Fagarasan, S., and T. Honjo. 2000. T-Independent immune response: new aspects of B cell biology. *Science* 290:89-92.
9.   Kidd, P. 2003. Th1/Th2 balance: the hypothesis, its limitations, and implications for health and disease. *Altern Med Rev* 8:223-246.
10.   Creagh, E. M., and L. A. O'Neill. 2006. TLRs, NLRs and RLRs: a trinity of pathogen sensors that co-operate in innate immunity. *Trends Immunol* 27:352-357.
11.   Lu, Y. C., W. C. Yeh, and P. S. Ohashi. 2008. LPS/TLR4 signal transduction pathway. *Cytokine* 42:145-151.
12.   Trinchieri, G. 2003. Interleukin-12 and the regulation of innate resistance and adaptive immunity. *Nat Rev Immunol* 3:133-146.
13.   Mazzoni, A., and D. M. Segal. 2004. Controlling the Toll road to dendritic cell polarization. *J Leukoc Biol* 75:721-730.
14.   Levings, M. K., S. Gregori, E. Tresoldi, S. Cazzaniga, C. Bonini, and M. G. Roncarolo. 2005. Differentiation of Tr1 cells by immature dendritic cells requires IL-10 but not CD25+CD4+ Tr cells. *Blood* 105:1162-1169.
15.   Banchereau, J., F. Briere, C. Caux, J. Davoust, S. Lebecque, Y. J. Liu, B. Pulendran, and K. Palucka. 2000. Immunobiology of dendritic cells. *Annu Rev Immunol* 18:767-811.

16. Wu, L., A. Nichogiannopoulou, K. Shortman, and K. Georgopoulos. 1997. Cell-autonomous defects in dendritic cell populations of Ikaros mutant mice point to a developmental relationship with the lymphoid lineage. *Immunity* 7:483-492.
17. Geissmann, F., M. G. Manz, S. Jung, M. H. Sieweke, M. Merad, and K. Ley. Development of monocytes, macrophages, and dendritic cells. *Science* 327:656-661.
18. Liu, K., and M. C. Nussenzweig. Origin and development of dendritic cells. *Immunol Rev* 234:45-54.
19. Kushwah, R., and J. Hu. Complexity of dendritic cell subsets and their function in the host immune system. *Immunology* 133:409-419.
20. Belz, G. T., and S. L. Nutt. Transcriptional programming of the dendritic cell network. *Nat Rev Immunol* 12:101-113.
21. den Haan, J. M., S. M. Lehar, and M. J. Bevan. 2000. CD8(+) but not CD8(-) dendritic cells cross-prime cytotoxic T cells in vivo. *J Exp Med* 192:1685-1696.
22. Heath, W. R., G. T. Belz, G. M. Behrens, C. M. Smith, S. P. Forehan, I. A. Parish, G. M. Davey, N. S. Wilson, F. R. Carbone, and J. A. Villadangos. 2004. Cross-presentation, dendritic cell subsets, and the generation of immunity to cellular antigens. *Immunol Rev* 199:9-26.
23. Dudziak, D., A. O. Kamphorst, G. F. Heidkamp, V. R. Buchholz, C. Trumpfheller, S. Yamazaki, C. Cheong, K. Liu, H. W. Lee, C. G. Park, R. M. Steinman, and M. C. Nussenzweig. 2007. Differential antigen processing by dendritic cell subsets in vivo. *Science* 315:107-111.
24. Belz, G. T., G. M. Behrens, C. M. Smith, J. F. Miller, C. Jones, K. Lejon, C. G. Fathman, S. N. Mueller, K. Shortman, F. R. Carbone, and W. R. Heath. 2002. The CD8alpha(+) dendritic cell is responsible for inducing peripheral self-tolerance to tissue-associated antigens. *J Exp Med* 196:1099-1104.
25. Proietto, A. I., M. H. Lahoud, and L. Wu. 2008. Distinct functional capacities of mouse thymic and splenic dendritic cell populations. *Immunol Cell Biol* 86:700-708.
26. Proietto, A. I., M. O'Keeffe, K. Gartlan, M. D. Wright, K. Shortman, L. Wu, and M. H. Lahoud. 2004. Differential production of inflammatory chemokines by murine dendritic cell subsets. *Immunobiology* 209:163-172.
27. Villadangos, J. A., and L. Young. 2008. Antigen-presentation properties of plasmacytoid dendritic cells. *Immunity* 29:352-361.
28. Barchet, W., M. Cella, and M. Colonna. 2005. Plasmacytoid dendritic cells--virus experts of innate immunity. *Semin Immunol* 17:253-261.
29. Jego, G., A. K. Palucka, J. P. Blanck, C. Chalouni, V. Pascual, and J. Banchereau. 2003. Plasmacytoid dendritic cells induce plasma cell differentiation through type I interferon and interleukin 6. *Immunity* 19:225-234.
30. Colonna, M., G. Trinchieri, and Y. J. Liu. 2004. Plasmacytoid dendritic cells in immunity. *Nat Immunol* 5:1219-1226.
31. Martin, P., G. M. Del Hoyo, F. Anjuere, C. F. Arias, H. H. Vargas, L. A. Fernandez, V. Parrillas, and C. Ardavin. 2002. Characterization of a new subpopulation of mouse CD8alpha+ B220+ dendritic cells endowed with type 1 interferon production capacity and tolerogenic potential. *Blood* 100:383-390.
32. Merad, M., and M. G. Manz. 2009. Dendritic cell homeostasis. *Blood* 113:3418-3427.
33. Serbina, N. V., T. Jia, T. M. Hohl, and E. G. Pamer. 2008. Monocyte-mediated defense against microbial pathogens. *Annu Rev Immunol* 26:421-452.
34. Geissmann, F., C. Auffray, R. Palframan, C. Wirrig, A. Ciocca, L. Campisi, E. Narni-Mancinelli, and G. Lauvau. 2008. Blood monocytes: distinct subsets, how they relate to dendritic cells, and their possible roles in the regulation of T-cell responses. *Immunol Cell Biol* 86:398-408.
35. Dominguez, P. M., and C. Ardavin. Differentiation and function of mouse monocyte-derived dendritic cells in steady state and inflammation. *Immunol Rev* 234:90-104.
36. Kurihara, T., G. Warr, J. Loy, and R. Bravo. 1997. Defects in macrophage recruitment and host defense in mice lacking the CCR2 chemokine receptor. *J Exp Med* 186:1757-1762.
37. Serbina, N. V., T. P. Salazar-Mather, C. A. Biron, W. A. Kuziel, and E. G. Pamer. 2003. TNF/iNOS-producing dendritic cells mediate innate immune defense against bacterial infection. *Immunity* 19:59-70.
38. Naik, S. H., P. Sathe, H. Y. Park, D. Metcalf, A. I. Proietto, A. Dakic, S. Carotta, M. O'Keeffe, M. Bahlo, A. Papenfuss, J. Y. Kwak, L. Wu, and K. Shortman. 2007. Development of plasmacytoid and conventional dendritic cell subtypes from single precursor cells derived in vitro and in vivo. *Nat Immunol* 8:1217-1226.
39. Carbone, F. R., G. T. Belz, and W. R. Heath. 2004. Transfer of antigen between migrating and lymph node-resident DCs in peripheral T-cell tolerance and immunity. *Trends Immunol* 25:655-658.
40. Helft, J., F. Ginhoux, M. Bogunovic, and M. Merad. Origin and functional heterogeneity of non-lymphoid tissue dendritic cells in mice. *Immunol Rev* 234:55-75.

41.	Merad, M., F. Ginhoux, and M. Collin. 2008. Origin, homeostasis and function of Langerhans cells and other langerin-expressing dendritic cells. *Nat Rev Immunol* 8:935-947.

42.	Dalod, M., and P. Pierre. Integration of ER stress and viral nucleotide sensing in DCs: mounting a response commensurate to the threat? *Eur J Immunol* 41:898-901.

43.	Berridge, M. J. 2002. The endoplasmic reticulum: a multifunctional signaling organelle. *Cell Calcium* 32:235-249.

44.	Brodsky, J. L., and W. R. Skach. Protein folding and quality control in the endoplasmic reticulum: Recent lessons from yeast and mammalian cell systems. *Curr Opin Cell Biol* 23:464-475.

45.	Ma, Y., and L. M. Hendershot. 2004. ER chaperone functions during normal and stress conditions. *J Chem Neuroanat* 28:51-65.

46.	Liu, C. Y., and R. J. Kaufman. 2003. The unfolded protein response. *J Cell Sci* 116:1861-1862.

47.	Kaufman, R. J. 2002. Orchestrating the unfolded protein response in health and disease. *J Clin Invest* 110:1389-1398.

48.	Harding, H. P., M. Calfon, F. Urano, I. Novoa, and D. Ron. 2002. Transcriptional and translational control in the Mammalian unfolded protein response. *Annu Rev Cell Dev Biol* 18:575-599.

49.	Kaufman, R. J. 1999. Stress signaling from the lumen of the endoplasmic reticulum: coordination of gene transcriptional and translational controls. *Genes Dev* 13:1211-1233.

50.	Schroder, M., and R. J. Kaufman. 2005. The mammalian unfolded protein response. *Annu Rev Biochem* 74:739-789.

51.	Todd, D. J., A. H. Lee, and L. H. Glimcher. 2008. The endoplasmic reticulum stress response in immunity and autoimmunity. *Nat Rev Immunol* 8:663-674.

52.	Walter, P., and D. Ron. The unfolded protein response: from stress pathway to homeostatic regulation. *Science* 334:1081-1086.

53.	Hosoi, T., and K. Ozawa. Endoplasmic reticulum stress in disease: mechanisms and therapeutic opportunities. *Clin Sci (Lond)* 118:19-29.

54.	Rutkowski, D. T., and R. J. Kaufman. 2007. That which does not kill me makes me stronger: adapting to chronic ER stress. *Trends Biochem Sci* 32:469-476.

55.	Hetz, C., and L. H. Glimcher. 2009. Fine-tuning of the unfolded protein response: Assembling the IRE1alpha interactome. *Mol Cell* 35:551-561.

56.	Schroder, M., and R. J. Kaufman. 2005. ER stress and the unfolded protein response. *Mutat Res* 569:29-63.

57.	Hetz, C., F. Martinon, D. Rodriguez, and L. H. Glimcher. The unfolded protein response: integrating stress signals through the stress sensor IRE1alpha. *Physiol Rev* 91:1219-1243.

58.	Lee, A. H., G. C. Chu, N. N. Iwakoshi, and L. H. Glimcher. 2005. XBP-1 is required for biogenesis of cellular secretory machinery of exocrine glands. *EMBO J* 24:4368-4380.

59.	Reimold, A. M., N. N. Iwakoshi, J. Manis, P. Vallabhajosyula, E. Szomolanyi-Tsuda, E. M. Gravallese, D. Friend, M. J. Grusby, F. Alt, and L. H. Glimcher. 2001. Plasma cell differentiation requires the transcription factor XBP-1. *Nature* 412:300-307.

60.	Bommiasamy, H., S. H. Back, P. Fagone, K. Lee, S. Meshinchi, E. Vink, R. Sriburi, M. Frank, S. Jackowski, R. J. Kaufman, and J. W. Brewer. 2009. ATF6alpha induces XBP1-independent expansion of the endoplasmic reticulum. *J Cell Sci* 122:1626-1636.

61.	Iwakoshi, N. N., M. Pypaert, and L. H. Glimcher. 2007. The transcription factor XBP-1 is essential for the development and survival of dendritic cells. *J Exp Med* 204:2267-2275.

62.	Martinon, F., X. Chen, A. H. Lee, and L. H. Glimcher. TLR activation of the transcription factor XBP1 regulates innate immune responses in macrophages. *Nat Immunol* 11:411-418.

63.	Hu, P., Z. Han, A. D. Couvillon, R. J. Kaufman, and J. H. Exton. 2006. Autocrine tumor necrosis factor alpha links endoplasmic reticulum stress to the membrane death receptor pathway through IRE1alpha-mediated NF-kappaB activation and down-regulation of TRAF2 expression. *Mol Cell Biol* 26:3071-3084.

64.	Martinon, F., and L. H. Glimcher. Regulation of innate immunity by signaling pathways emerging from the endoplasmic reticulum. *Curr Opin Immunol* 23:35-40.

65.	Hu, F., X. Yu, H. Wang, D. Zuo, C. Guo, H. Yi, B. Tirosh, J. R. Subjeck, X. Qiu, and X. Y. Wang. ER stress and its regulator X-box-binding protein-1 enhance polyIC-induced innate immune response in dendritic cells. *Eur J Immunol* 41:1086-1097.

66.	Yoshida, H. 2007. ER stress and diseases. *FEBS J* 274:630-658.

67.	Lee, A. H., E. F. Scapa, D. E. Cohen, and L. H. Glimcher. 2008. Regulation of hepatic lipogenesis by the transcription factor XBP1. *Science* 320:1492-1496.

68.	Hornbeck, P., S. E. Winston, and S. A. Fuller. 2001. Enzyme-linked immunosorbent assays (ELISA). *Curr Protoc Mol Biol* Chapter 11:Unit11 12.

69.   Hess, D. A., S. E. Humphrey, J. Ishibashi, B. Damsz, A. H. Lee, L. H. Glimcher, and S. F. Konieczny. Extensive pancreas regeneration following acinar-specific disruption of Xbp1 in mice. *Gastroenterology* 141:1463-1472.

70.   Hosokawa, N., I. Wada, Y. Natsuka, and K. Nagata. 2006. EDEM accelerates ERAD by preventing aberrant dimer formation of misfolded alpha1-antitrypsin. *Genes Cells* 11:465-476.

71.   Pilon, M., R. Schekman, and K. Romisch. 1997. Sec61p mediates export of a misfolded secretory protein from the endoplasmic reticulum to the cytosol for degradation. *EMBO J* 16:4540-4548.

72.   Bauer, D. E., V. Haroutunian, R. E. McCullumsmith, and J. H. Meador-Woodruff. 2009. Expression of four housekeeping proteins in elderly patients with schizophrenia. *J Neural Transm* 116:487-491.

73.   Iwakoshi, N. N., A. H. Lee, P. Vallabhajosyula, K. L. Otipoby, K. Rajewsky, and L. H. Glimcher. 2003. Plasma cell differentiation and the unfolded protein response intersect at the transcription factor XBP-1. *Nat Immunol* 4:321-329.

74.   Baxi, S. N., and W. Phipatanakul. The role of allergen exposure and avoidance in asthma. *Adolesc Med State Art Rev* 21:57-71, viii-ix.

75.   Jacquet, A. 2009. New insights into the molecular basis of the house dust mite-induced allergic Response. *The Open Allergy Journal* 2:38-44.

76.   Maddur, M. S., J. Vani, J. D. Dimitrov, K. N. Balaji, S. Lacroix-Desmazes, S. V. Kaveri, and J. Bayry. 2010. Dendritic cells in autoimmune diseases. *The Open Arthritis Journal* 3:1-7.

77.   Blanco, P., A. K. Palucka, V. Pascual, and J. Banchereau. 2008. Dendritic cells and cytokines in human inflammatory and autoimmune diseases. *Cytokine Growth Factor Rev* 19:41-52.

78.   Willart, M., and H. Hammad. Lung dendritic cell-epithelial cell crosstalk in Th2 responses to allergens. *Curr Opin Immunol* 23:772-777.

79.   Kaser, A., A. H. Lee, A. Franke, J. N. Glickman, S. Zeissig, H. Tilg, E. E. Nieuwenhuis, D. E. Higgins, S. Schreiber, L. H. Glimcher, and R. S. Blumberg. 2008. XBP1 links ER stress to intestinal inflammation and confers genetic risk for human inflammatory bowel disease. *Cell* 134:743-756.

Nederlandse samenvatting

Endoplasmatisch reticulum (ER) stress wordt veroorzaakt door verstoringen die de eiwitopvouwing van het ER in gedrang brengen en leiden tot accumulatie van niet-opgevouwen eiwitten. Om de stress te overleven, activeren de cellen de 'unfolded protein response' (UPR), die transcriptionele en translationele processen aanpast aan de huidige staat van eiwitopvouwing. ER stress neemt zo af doordat enerzijds de input van nieuw gevormde eiwitten wordt verhinderd en verkeerd opgevouwen eiwitten worden gedegradeerd, en anderzijds door de opregulatie van de transcriptie van chaperones in het ER. De UPR bestaat uit drie ER stress sensoren waaronder IRE1 het meest geconserveerd is. Het activeert de transcriptiefactor XBP1 om zo de expressie van ER stress gerelateerde genen te induceren. Recent werd ontdekt dat XBP1 essentieel is voor de ontwikkeling en overleving van plasmacytoide en conventionale dendritische cellen (DCs), een kenmerk dat tot dan toe enkel was beschreven voor plasmacellen en secretoire cellen.

In deze masterproef wordt onderzoek gedaan naar de rol van XBP1 in de overleving, maturatie, functie en management van ER stress in DCs. Er werd gebruik gemaakt van het CD11c Cre-LoxP systeem om een muismodel te creëren met een DC-specifieke deletie van het XBP1 gen en inflammatoire DCs (iDCs) werden verkregen na 8 dagen cultuur van beenmerg cellen in aanwezigheid van de groeifactor granulocyte-macrophage colony-stimulating factor (GM-CSF). Om overleving te promoten, werden de DCs gestimuleerd met verschillende pathogen recognition receptor (PRR) liganden. Ook werd de capaciteit van deze PRR stimuli om ER stress te triggeren, onderzocht.

Onze resultaten wijzen op een link tussen specifieke PRR-pathways en de UPR in iDCs, gezien stimulatie met lipopolysaccharide (LPS), huisstofmijt (HDM), CpG oligodeoxynucleotiden en curdlan een opregulatie van ER stress genen induceerde. We konden geen essentiële rol voor XBP1 in de overleving van iDCs aantonen, gezien het percentage aan levende cellen slechts een weinig gedaald was in XBP1-deficiënte iDCs.

Ook de expressie van co-stimulatoire molecules (CD40 en CD86), wat een indicator is voor de maturatie status, bleek niet verschillend te zijn tussen beide groepen. XBP1 zou dus niet essentieel zijn voor de maturatie van iDCs, hoewel de capaciteit van iDCs om cytokines te secreteren wel verschillend was in beide groepen. Zo secreteerden de iDCs in afwezigheid van XBP1 minder cytokes en dit effect was ligand- en cytokine-specifiek, met IL-6 en IL-12 zijnde het meest beïnvloed na stimulatie met LPS en HDM. Algemeen kunnen we concluderen dat de IRE1-XBP1 signaalbaan geen eenduidige rol speelt in iDCs.